



## GEOCHEMISTRY OF THE KIZILDERE-TEKKEHAMAM- BULDAN- PAMUKKALE GEOTHERMAL FIELDS, TURKEY

**Ali Gökgöz**

Pamukkale University, Engineering Faculty,  
The Department of Geological Engineering  
20017, Denizli  
TURKEY

### ABSTRACT

The Kizildere and neighbouring geothermal fields are located in the Büyük Menderes and Gediz grabens and the intersection of these grabens. The chemical composition of waters in the study area is governed by rock-water interaction, but does not reflect a peripheral or steam-heated origin. The geothermometry temperatures for Kizildere well waters vary between 188 and 245°C. By comparison with measured temperatures in drillholes at Kizildere, it is concluded that subsurface temperature in the Kizildere and Tekkehamam areas must be quite similar. In other areas, reservoir temperatures are relatively low. The waters of the Buldan and Pamukkale groups are immature to partly equilibrated; the Tekkehamam and Kizildere waters have evolved close to full equilibrium.

The scaling in Kizildere wells is a major problem and causes decline in well productivity. The main scale formation in the wells is calcite. In the flashing zone, loss of CO<sub>2</sub> leads to increased pH and strong supersaturation with respect to calcite and subsequent precipitation of this mineral. The water discharged from Kizildere wells is also supersaturated with respect to calcite. It is the increase in CO<sub>3</sub><sup>-2</sup> and Ca<sup>+2</sup> concentrations associated with the boiling, degassing, and cooling of the aquifer waters that is responsible for the produced calcite supersaturation.

Various data such as the linear relationship between δ<sup>18</sup>O and Cl, between Cl and B, and the plots on the Na-K-Mg diagram indicate that mixing has taken place between cold and hot water in the upflow zones. The silica-enthalpy and the chlorine-enthalpy mixing models were applied to estimate subsurface temperatures in the study area and gave similar reservoir temperatures as those of the chemical geothermometers.

### 1. INTRODUCTION

Turkey is located on an active tectonic belt with many tectonic structures such as faults, grabens, overthrusts, folds, and widespread acidic volcanism, hydrothermal alteration zones and geothermal areas. Figure 1 shows the general tectonic and volcanic features of Turkey. Most of the geothermal areas in

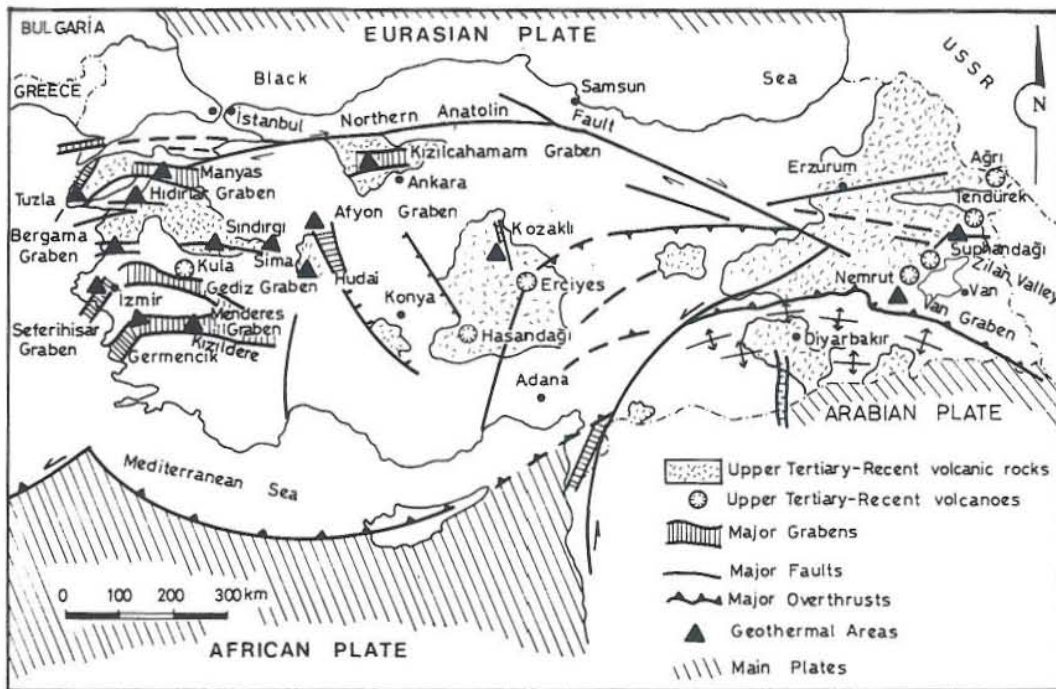


FIGURE 1: General tectonic and volcanic features of Turkey (Simsek, 1985a)

Turkey are located in the western part of Anatolia where geological and hydrogeological conditions are favourable for the formation of geothermal systems, whereas the regional tectonic structures are more widespread (Figure 1).

The main high-enthalpy geothermal fields in Turkey are the Kizildere (200-240°C), Omerbeyli-Germencik (232°C), Canakkale-Tuzla (174°C), Simav-Kütahya (165°C) and İzmir-Seferihisar (145°C) geothermal fields, whereas there are a lot of low-enthalpy fields. All of the available data indicates that Turkey has a very important geothermal energy potential.

Geothermal exploration for electricity production purposes have focused on the Kizildere-Tekkehamam area owing to its high potential. The Directory of Mineral Research and Exploration (MTA) started to explore the field in 1960 with support from the United Nations Development Programme (UNDP). The first major geothermal power plant in Turkey, which was built by the Turkish Electricity Authority (TEK) and has been operated by TEK (later renamed to TEAS) to the present, was commissioned in Kizildere in 1984, with an installed capacity of 20.4 MW. At present Turkey produces geothermal heat enough for 50,000 houses and greenhouses of 200,000 m<sup>2</sup> with 350 MWt, and 190 hot springs with 285 MWt, totalling 635 MWt, and 20.4 MWe (S. Simsek, personal communication). The present study focuses on geochemical interpretation of chemical data on waters from cold, warm, hot and boiling springs, and wells in the Kizildere and neighbouring geothermal fields, W-Turkey.

Geothermal fluids ascending from a geothermal reservoir and emerging at the surface provide information about subsurface conditions. Geochemistry furnishes one of the most economical and efficient methods to assess origin, subsurface temperature, equilibrium states of thermal fluids and such problems as scaling. It also helps determine probable mixing processes, using conservative constituents which dissolve from rocks but are not precipitated or ion-exchanged such as Cl, B, Li, or geo-indicators, chemically reactive species which change with changing conditions like Na, K, Ca, Mg and SiO<sub>2</sub>, or stable isotopes of water e.g. <sup>18</sup>O and deuterium, and unstable isotopes like tritium.

In this report, special emphasis is put on the study of the origin of the geothermal water, water-rock interaction, the mixing of geothermal with colder fluids in upflow zones, and mineral saturation. The results obtained by various chemical geothermometers are compared with temperatures estimated using different mixing models. A new approach has been taken to assess the scaling problem in the Kizildere area.

## **2. GENERAL OUTLINE OF THE KIZILDERE AND NEIGHBOURING GEOTHERMAL FIELDS**

### **2.1 Geological setting**

In the thermal fields of Kizildere-Tekkehamam-Buldan-Pamukkale, the basement rocks are Paleozoic Menderes metamorphics which are characterized by alternations of marble, calcschist, quartzite and schist (the İğdecik formation; Simsek, 1985a), schist and gneiss. The basement is overlain by Pliocene sediments which have continental and lacustrine characteristics. These sediments have been divided into four lithologic units (Simsek, 1985a). From bottom to top these units are: (1) Kizilburun formation which is composed of alternating red and brown conglomerates, sandstones and claystones, and lignite seams. Its thickness is about 200 m. (2) Sazak formation which consists of intercalated gray limestones, marls and siltstones, 100 to 250 m thick. (3) Kolankaya formation composed of alternating layers of sandstone, claystone and clayey limestone, the thickness is about 500 m. (4) The Tosunlar formation which is characterized by poorly consolidated conglomerates, sandstones and mudstones with fossiliferous claystone, the thickness reaches up to 500 m. The first three mentioned units are Lower Pliocene in age whereas the Tosunlar formation is Plio-Quaternary and overlies the Lower Pliocene and Paleozoic rocks and is separated from them by angular unconformity. The Quaternary formation consists of terrace deposits, alluvium, slope debris, alluvial fans and travertine. Figures 2 and 3 present geological map of the study area with the distribution of geothermal manifestations and the block diagram of geology of the Kizildere-Tekkehamam-Buldan geothermal field, respectively.

The collision between the Anatolian and Arabian plates started westward movement of the Anatolian plate along the North Anatolian and East Anatolian Faults during the Middle Miocene. Impediments of this movement by the Greek Shearing zone created E-W compression in the Menderes Massif which in turn led to a N-S extension and the formation of graben systems in the Aegean geographical region of Turkey. The driving force of the extension is the subduction of the north African oceanic crust beneath the westward moving Anatolian plate along the Hellenic Trench (Sengör and Yilmaz, 1981). The length and the depth of the Hellenic Trench are 1550 km and 3 km, respectively, and the rate of subduction is 2.7 cm/year (Toksöz, 1975).

### **2.2 Surface manifestations and hydrogeology**

In the topographic lows in Kizildere and Tekkehamam, several fumeroles are found on the mountain slopes and hot springs with temperatures ranging between 30 and 100°C. The hot springs issue at the point where faults cut the valley. These springs deposit travertine and alteration minerals along the fault lines and in the vicinity of the springs.

The temperature of the hot springs which ascend to the surface through faults related to the Gediz graben in the Buldan area are in the range of 36-57°C. In this area the main type of deposition from the geothermal fluid is travertine.

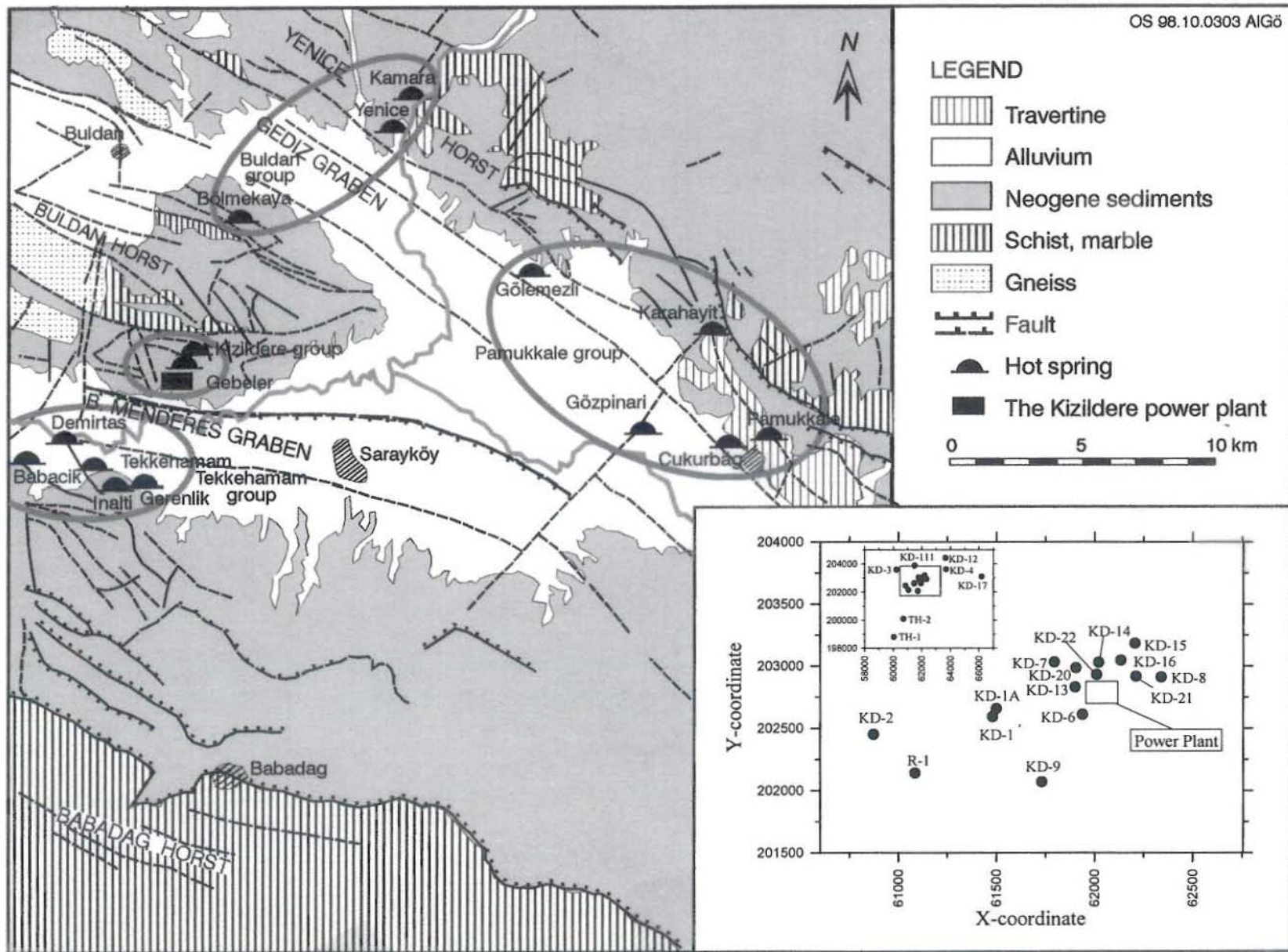


FIGURE 2: Geological map of the study area and location of the geothermal fields (modified from MTA)

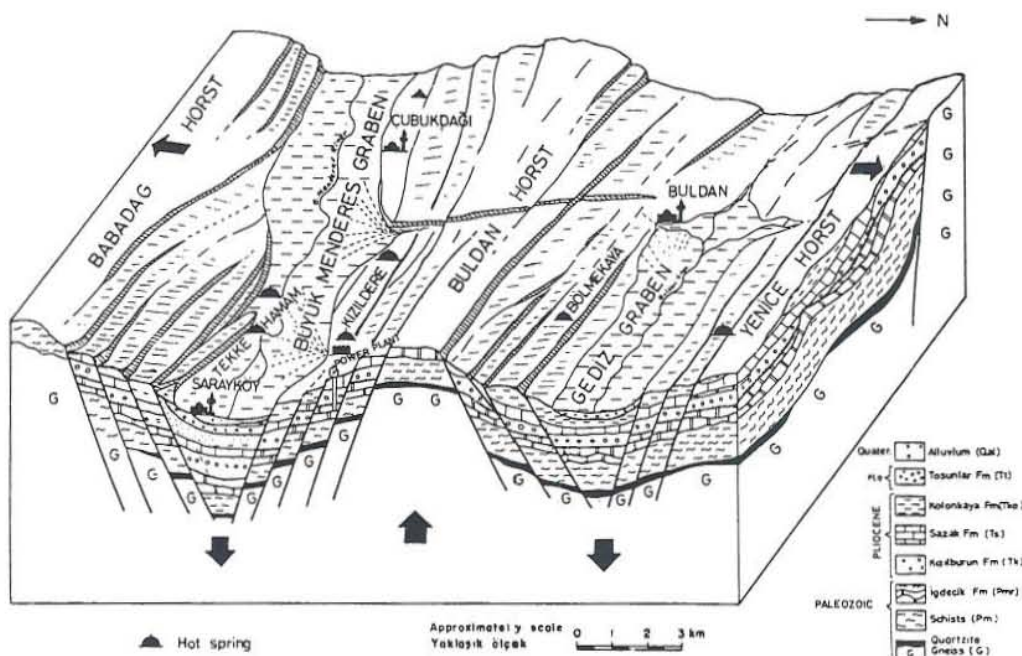


FIGURE 3: Block diagram of the Saraykoy-Buldan area (from Simsek, 1985a)

The hot springs of Pamukkale (group) are located at the intersection of the Büyük Menderes and Gediz grabens. Their temperature is in the range of 28-59°C. In this area the thickness of travertine reaches 85 m. The Pamukkale springs, which have a temperature of 36°C, deposit snow white travertine, whereas the Kizilleğen spring deposits red travertine due to high iron concentrations in the fluid. Pamukkale and Karahayit are tourist attractions, visited by 1.5 million tourists every year. Some environmental problems are associated with tourism as well as with the exploitation of wells in the area, causing a decrease in flowrate and temperature of springs and pollution of the white travertine.

A schematic model for the Kizildere and Tekkehamam geothermal fields, by Simsek (1985a), is shown in Figure 4. The model is supported by temperature and pressure data for the Kizildere geothermal area.

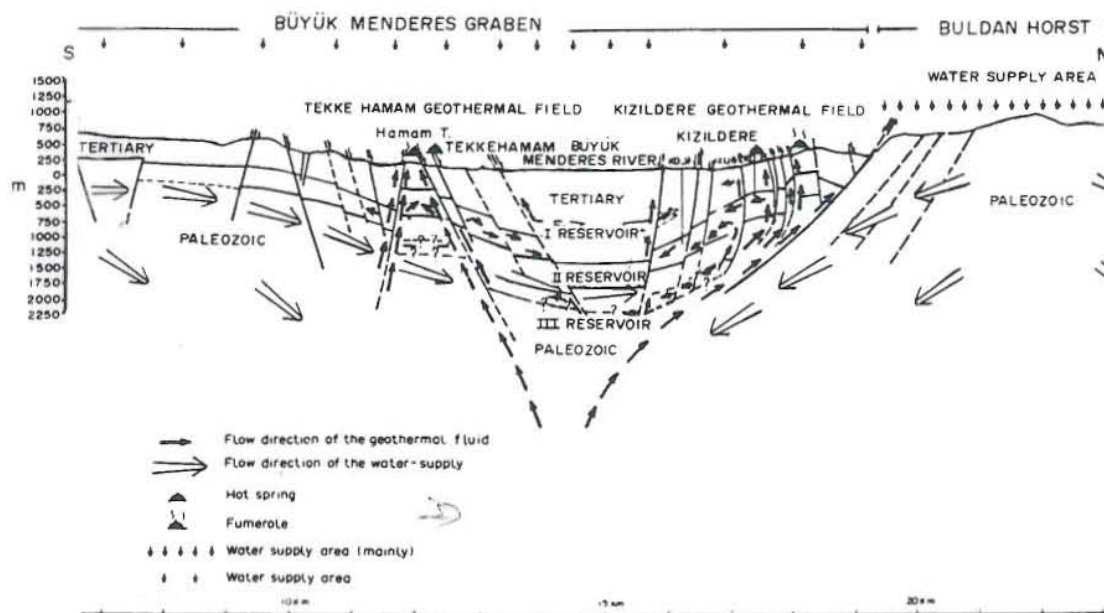


FIGURE 4: Cross-section of the hydrothermal system in the Kizildere-Tekkehamam geothermal areas (Simsek, 1985a)

**Heat source:** Young volcanic activity exists in the region as witnessed by the Kula volcanics. There are, however, no volcanic rocks in the vicinity of Kizildere. Volcanism near Kizildere is closely related to the rift system (Ercan, 1979). The plate tectonics models proposed for Turkey involve mantle uplift, particularly below the Menderes massif (Arpat and Bingöl, 1969; Alptekin, 1973; Bingöl, 1976; Kaya, 1981). A heat flow map of the region reveals high heat flow anomalies along the grabens (Tezcan, 1979) probably due to magmatic intrusions. Filiz (1982) suggested that the origin of CO<sub>2</sub> gas in Pamukkale springs is magmatic. Gülec (1988) revealed that helium-3 in the regional waters is of mantle origin. According to these data, meteoric waters which percolate deep into the crust gain heat from magmatic intrusions and from magmatic emanations from the intrusions.

**Reservoir rock:** The rocks of the Kizildere geothermal reservoir are of three types. At the shallowest level there are limestones of limited lateral extent of the Pliocene Sazak formation. Compared with other reservoir rocks, the limestones have low porosity, low permeability and low temperature, about 180°C. Thickness varies between 100 and 250 m (Simsek, 1985a). Under the Pliocene Sazak limestones are alternations of marble-quartzite-schist of the İğdecik formation which have relatively high porosity and permeability. Average temperature is 202°C and thickness varies between 100 and 300 m. Analysis of pressure profiles measured in the wells prior to exploitation shows a hydrostatic pressure connection between aquifers in the first and second formations. Therefore, they must be considered as the same hydrological system or reservoir (Okandan, 1988). The deepest lithological unit of the Kizildere reservoir consists of quartzite. According to data from well R-1, it has good permeability and high temperature (242°C); (İ.H. Karamanderesi, personal communication).

**Aquicludes:** There are three aquicludes in the Kizildere system which are composed from top to bottom of impermeable layers of the Kolankaya formation and consist of alternating well-consolidated conglomerates, sandstones and claystones of the Kizilburun formation and schist of the Menderes metamorphics. The hydrogeological units are summarized in Table 1.

**Recharge:** Recharge is mainly meteoric and involves surface- and underground waters infiltrating the basin. The geothermal fluid ascends to the productive aquifers through the major faults bounding the grabens after being heated at greater depths. It is then drained towards the centre of the graben where it mixes with cold groundwater (Simsek, 1985a).

The general features of the geothermal model for the Kizildere field, just described, are also valid for other geothermal fields in the study area.

TABLE 1: Hydrogeological units for the Kizildere geothermal area (modified from Simsek, 1985a)

Formation	Lithology	Thickness	Hydrological feature
Alluvium	Block, gravel, sand, silt and clay	Variable	Permeable
The Tosunlar formation	Poorly consolidated conglomerates, sandstones, mudstones and claystones	max. 500 m	Weakly permeable
The Kolankaya formation	Alternations of sandstone, claystone and clayey limestone	500 m	Aquiclude
The Sazak formation	Intercalated limestones, marls and siltstones	100-250 m	Limestones are topmost reservoir rocks
The Kizilburun formation	Alternations of conglomerates, sandstones and claystones	200 m	Aquiclude
The İğdecik formation	Alternations of marble, chertschist, quartzite and schist	100-300 m	Permeable Intermediate reservoir
Schists	Various schist	-	Aquiclude
Gneiss	Quartzitic gneiss	150 m with upper part	Highly permeable, deepest reservoir (quartzite)



FIGURE 5: Denizli-Saraykoy area, the second-derivate of the gravity map (Tezcan, 1967)

### 2.3 Geophysical measurements

Geophysical investigations including gravity, resistivity, seismic measurements and geothermal gradient surveys have been carried out to obtain information about underground geology such as the thickness and distribution of the aquicludes and aquifers.

The gravity studies carried out in the Denizli-Saraykoy area (Tezcan, 1967; Ekingen, 1970) yielded information about the major tectonic structures in the area and establishment of the tectonic skeleton of the area. The position of convergence of the gravity lines trending E-W are related to step faulting (Figure 5).

The resistivity measurements in the Kizildere and Tekkehamam geothermal areas were carried out in order to construct resistivity maps at 70-900 m depth (Tezcan, 1967). From the measured resistivity values it can be seen that resistivity is low both in the Kizildere area and the Tekkehamam area. It increases to the north in Kizildere and to the south in Tekkehamam. The areas with a resistivity below 5  $\Omega$ m values are considered the most suitable areas for drilling.

A total of 130 gradient boreholes have been drilled to depths between 80 and 250 m in the Kizildere and Tekkehamam geothermal fields. About 100 boreholes were drilled in Kizildere and another 30 in Tekkehamam (Demirorer, 1967; Simsek and Yilmazer, 1977). The measured temperatures in the wells give gradient values between 10 and 100°C/100 m. The highest values recorded within Kizildere and Tekkehamam are 92 and 110°C/100 m, respectively, while the lowest values in these fields are about 30°C/100 m.

### 2.4 Drilling history

Following the geological, geophysical and geochemical surveys, which yielded positive results, the first production wells KD-1 and TH-1 were drilled by UNDP and MTA in 1968. Well KD-1, located in Kizildere was drilled to a depth of 540 m and it produced a mixture of water and steam of 198°C from the shallowest aquifer. The well proved the existence of a geothermal reservoir with a temperature of about 200°C. Well TH-1 was drilled to 615 m depth and it penetrated the uppermost aquifer. But the measured temperature at the bottom of the well was only 116°C, indicating that reservoir temperatures

in the Tekkehamam geothermal field were much lower than at Kizildere. For that reason, drilling continued in Kizildere. Well KD-1 indicated quite high temperatures and deeper wells might reveal even higher.

During 1968-1975, a total of 16 wells were drilled in Kizildere. Some of them (KD-1, KD-1A, KD-2, KD-3, KD-4, KD-8, KD-12, KD-17 and KD-111) were drilled to shallow depths and only penetrated the topmost aquifer. The depth of these wells is in the range of 370-706 m. The measured bottom well temperature ranges between 148 and 190°C. Wells KD-6, KD-7, KD-9, KD-13, KD-14, KD-15 and KD-16 penetrated the second aquifer. The depths and bottom well temperatures of these wells are in the range 365-1241 m and 172-211°C, respectively. The average temperature for this part of the reservoir is 202°C.

Later, two reinjection wells (TH-2 and R-1) were drilled in the area. Well TH-2 was drilled in 1996 to 2000 m depth about 6 km from the power plant. The well penetrated the topmost aquifer at 548-633 m, second aquifer at 815-905 m and schist and gneiss below 905 m depth. The drill mud temperature in the well was measured as 147°C at 1701 m depth. Results of well tests indicated that the well was not suitable for reinjection. Well R-1, which is located between wells KD-2 and KD-9, was completed to a depth of 2261 m with 242°C in early 1998. Well testing is still in progress. A summary of the wells in the area is given in Table 2.

TABLE 2: Basic information about wells in the study area (from Simsek, 1985b; Tan, 1985; ENEL et al., 1989), \*average values in March 1994

Well No.	Drilling period	Depth (m)	Elevation (m)	Temp. (°C)	WHP* (kg/cm <sup>2</sup> )	Flow* (tonnes/h)	Comments
KD-1	20.4-12.5.68	450	177.08	198	-	-	Leakage
KD-1/A	17.1-15.2.69	451.5	183.53	195	-	-	
KD-2	16.9-8.11.68	706.5	169.79	174	-	-	Monitoring
KD-3	26.3-25.4.69	370	345.28	172	-	-	
KD-4	7.5-26.10.69	486	364.36	178	-	-	
KD-111	1.7-25.10.69	504.8	456.39	152	-	-	
KD-6	19.11.69-27.1.70	851	184.01	196	13.5	78.2	Producer
KD-7	6.7-8.8.70	667.5	203.15	208	-	-	Producer/Monitor
KD-8	6.5-9.6.70	576.5	210.84	190	-	-	Leakage/Monitor
KD-9	1.2-16.3.70	1241	156.35	172	-	-	Monitoring
KD-12	25.4-17.6.70	404.7	294.46	148	-	-	Dry
KD-13	23.3-23.4.71	760	189.29	195	13.7	75	Producer
KD-14	2.11-29.11.71	597	197.02	207	14.4	122.8	Producer
KD-15	9.5-31.5.71	506.2	211.05	205	15	115	Producer
KD-16	29.4-9.6.73	365.2	199.05	211	14.9	161.7	Producer
KD-17	28.7-7.8.75	666.5	201.76	-	-	-	
KD-20	19.12.85-21.1.86	810	194.6	201	13.7	123.7	Producer
KD-21	14.10-29.11.85	897.5	204.89	202	12.7	88.9	Producer
KD-22	25.6-27.8.85	887.5	193.35	202	13.3	94.7	Producer
TH-1	27.1-19.12.68	615.5	151.15	116	-	-	
TH-2	1996	2000	131.87	147	-	-	
R-1	1998	2261	148.36	242	-	-	



## 2.5 Utilization

As mentioned above, 16 wells were drilled in Kizildere from 1968 to 1975. Some fluid was produced from these wells during this period to test their capacity, particularly during 1972-1973 (Tan, 1985).

Small scale utilization of the field started in 1975 when a small backpressure steam turbine (0.5 MW) was installed in Kizildere. The geothermal fluid was supplied to the turbine from well KD-13. The produced electricity was distributed to a village in the area.

Another flow test of one year duration was carried out in 1976-1977 (Tan, 1985). The total fluid produced during this year was 5.4 Mtonnes from wells KD-6, KD-7, KD-14, KD-15 and KD-16. A report prepared by MTA concluded that six wells in Kizildere were suitable for electricity production. After a feasibility study carried out by TEK, a power plant was erected at Kizildere with an installed capacity of 20.4 MW. Construction was completed in February, 1984. The net contribution from the plant to the national transmission system is 17.8 MW. Three new wells were added in 1985-1986 in order to increase production from the reservoir. For the last ten years the plant has only been producing about 10 MW. The annual power production of Turkey is 106,520 GWh whereas the annual production of the geothermal plant is 90 GWh or 0.85% of total power production in Turkey.

About 900 tonnes/h of geothermal fluid is produced from the reservoir. About 90% of this fluid, at 148°C, is discharged into the Büyük Menderes river through a waste water channel. The geothermal effluent of Kizildere is very high in boron and unacceptable for irrigation. So, during the main irrigation period in September and October, the power plant has to be shut down for about 20 days for the last few years, due to high influence on the water in the river. In the near future it is hoped that reinjection wells and the geothermal district heating project for Denizli will solve these problems.

The fluid in the reservoir in the Kizildere geothermal area has a CO<sub>2</sub> content of about 2%. At the separator pressure (70 psig), it contains about 12-20% steam and about 10-20% of the steam is non-condensable gases, mainly CO<sub>2</sub>. The CO<sub>2</sub> gas is used to produce dry ice (dry CO<sub>2</sub>) by the Karbogaz A.S. company. Installed capacity of the dry ice factory is 40,000 t/year. The dry ice produced in the factory is sufficient for 90-95% of the market in Turkey. The surface area of the greenhouses in Kizildere is 8000 m<sup>2</sup>. Tomatoes, cucumbers and several flowers are grown in these greenhouses. The other main types of utilization of geothermal energy in the Kizildere-Tekkehamam-Buldan-Pamukkale areas include bathing, health spas, swimming pools and scenery such as Pamukkale travertines.

## 3. GEOTHERMAL DATA

The present geochemical study is based on 30 samples selected from hot springs, boiling springs, wells, waste water from the Kizildere power plant, and cold water from the area. The chemical and isotopic composition of the samples is shown in Table 3 and location in Figure 2. These waters were divided into four geographical groups except for the cold water.

1. The Kizildere group consist of water from the Kizildere wells, Kizildere hamami and Gebeler deresi.
2. The Tekkehamam group is composed of water from well TH-1, Demirtaş, Tekkehamam, İnalti mağarasi, Babacik and Gerenlik gölü springs.
3. The Buldan group includes water from Bolmekaya, Yenice hamami and Kamara hot springs.
4. The Pamukkale group consists of water from Pamukkale, Cukurbag, Kizilleğen and Gölemezli springs.

TABLE 3: Analytical results for waters from Kizildere, Tekkehamam, Buldan and Pamukkale areas, concentrations in ppm

No.	Well or spring	Date	T <sub>meas</sub> (°C)	pH/°C	EC (µS/cm)	Na	K	Ca	Mg	Fe (tot)	Al	Li	B (tot)	SiO <sub>2</sub>	CO <sub>2</sub> (tot)	Cl	SO <sub>4</sub>	F	Ionic bal. % diff.	δ <sup>18</sup> O (‰)	δD (‰)	Tritium (T.U)
<b>Kizildere group</b>																						
KD-6*	Well KD-6	14.04.1996	196	8.97/25	5830	1220	116	1.2	0.36	-	-	3.96	20.4	364	1150.1	124	560	17.8	22.41	-6.03	-53.8	14-28
KD-13*	Well KD-13	14.04.1996	195	8.89/25	5940	1300	138	2.0	0.23	-	-	4.09	26.5	364	1103.5	128	773	20.0	22.62	-5.53	-54.1	14-28
KD-14*	Well KD-14	14.04.1996	207	8.96/25	6160	1410	152	1.2	0.20	-	-	4.45	24.4	392	1745.9	144	737	24.8	0.52	-	-	-
KD-15*	Well KD-15	14.04.1996	205	8.82/25	5890	1340	138	1.2	0.15	-	-	3.62	24.6	393	1059.1	140	730	22.3	28.72	-	-	-
KD-16*	Well KD-16	14.04.1996	211	8.94/25	5835	1400	148	3.2	0.24	-	-	4.43	24.0	398	1103.8	136	714	23.5	29.24	-	-	-
KD-20*	Well KD-20	14.04.1996	201	8.92/25	6180	1375	140	1.6	0.15	-	-	4.58	24.1	367	836.5	140	710	22.5	43.68	-	-	-
KD-21*	Well KD-21	14.04.1996	202	9.02/25	5940	1325	131	1.8	0.24	-	-	-	24.5	387	880.7	140	710	21	35.22	-	-	-
KD-22*	Well KD-22	14.04.1996	202	9.30/25	5830	1275	140	1.2	0.24	-	-	-	25.0	392	1148.2	136	729	22.5	11.17	-	-	-
W-1*	Waste water	14.04.1996	92	9.25/25	5500	1400	138	1.2	0.60	-	-	-	26.0	345	970.1	136	735	21.7	29.35	-	-	-
1**	Kizildere hamami	08.06.1976	100	7.90/20	3700	1200	110	5.1	1.40	0.00	-	-	21.0	140	1484.4	100	680	13	8.57	-	-	-
2**	Gebeler deresi	08.06.1976	100	8.00/20	3700	1300	112	13	1.20	0.00	-	-	22.4	236	1617.7	111	812	18.5	4.55	-	-	-
<b>Tekkehamam group</b>																						
TH-1*	Well TH-1	10.1987	116	7.71/25	4000	750	75	12	12	-	-	1.62	12.1	210	334.9	76	1350	8.3	-5.51	-	-	-
3**	Demirtaş	10.05.1976	98	6.70/20	2600	650	46	50	16	0.88	-	-	15.0	198	642.3	74	1030	7.5	-2.77	-	-	-
4**	Tekkehamam	19.04.1976	99	7.60/20	3700	995	95	16	3.4	0.26	-	-	19.0	120	970.2	102	1230	14	-7.33	-6.52	-55.9	33±10
5**	Tekkehamam-1	08.06.1970	60	7.90/20	3800	530	64	210	53	0.60	-	-	-	210	1155.1	90	1070	0.0	-27.07	-	-	-
6**	Tekkehamam-2	13.05.1976	72	7.70/20	3800	984	99	45	15	1.30	-	-	20.0	160	1036.5	97	1190	13.0	-4.42	-	-	-
7**	İnalti mağarası	31.05.1976	55.5	6.45/20	-	735	73	186	35	0.00	-	-	13.0	375	728.8	87	1700	6.0	-4.15	-	-	-
8**	Babacık pinarı	10.05.1976	61.5	6.20/20	2930	500	46	260	79	0.26	-	-	9.80	150	1289.7	62	1390	6.3	-3.91	-	-	-
9**	Gerenlik gölü	10.05.1976	73.5	7.10/20	3680	1000	94	30	1.0	0.30	-	-	20.0	210	1474.0	110	1070	12	-14.30	-	-	-
<b>Buldan group</b>																						
10**	Bölmekaya	25.01.1976	36	7.40/20	1020	23.5	9.8	1.5	77	0.14	-	-	2.20	100	341.2	18	342	1.6	-70.76	-	-	-
11**	Yenice hamami	10.05.1976	40.8	5.80/20	1950	260	42	300	36	7.00	-	-	3.20	100	4840.4	34	350	2.6	-11.50	-8.16	-52.2	29±9
12**	Kamara	10.05.1976	56.8	6.70/20	2900	580	86	290	42	1.70	-	-	5.70	120	1956.5	51	720	2.3	-6.47	-8.67	-56.9	14-28
<b>Pamukkale group</b>																						
13#	Pamukkale	27.06.1993	35.5	6.30/35	1990	39	5.0	406	96	0.07	0.16	0.08	0.30	34	1496.1	21	822	1.0	-22.46	-10.00	-58.5	14-28
14**	Cukurbağ	10.05.1976	59	7.70/20	-	130	22	530	110	1.40	-	-	2.70	43	1070.9	34	830	2.5	-0.74	-	-	-
15**	Gozpinari	01.06.1976	28	6.40/20	-	54	8.4	390	104	0.00	-	-	2.30	63	1295.7	20	728	2.0	-5.44	-	-	-
16#	Karahayit-	24.02.1992	54.5	6.13/20	2500	120	22	483	114	0.13	0.19	0.3	1.00	39	2278.6	28	944	2.0	-6.64	-9.14	-56.6	14-28
17#	Kizilleğen	24.02.1992	50.4	5.90/20	4000	560	60	379	121	0.32	0.21	1.86	21.0	161	3594.2	89	1662	2.3	-20.95	-8.54	-56.2	14-28
18#	Gölemezli hamami Gölemezli kaynağı	24.07.1992	48.4	6.32/20	4128	517	49	340	156	0.14	0.19	1.82	10.0	122	1716.3	84	1533	2.0	-7.34	-	-	-
<b>Cold water</b>																						
19*	Cold water-1	10.1987	16.6	7.60/20	550	11.9	1.5	65	1.0	-	-	-	0.3	27	183.9	7.5	23	1.7	-25.87	-	-	-
20*	Cold water-2	10.1987	15.3	7.60/20	850	44.8	0.9	72	5.2	-	-	-	0.5	52	347.6	7.0	108	1.8	-51.69	-	-	-

References for selected samples: \* Yildirim et al. 1997; \*\* Simsek, 1982; # Gökğöz, 1994; isotope analysis (sampling date 15.02.1979), taken from Filiz 1982

The coordinates of the wells in the Kizildere geothermal area were taken from MTA. The analytical data given in Table 3 were gathered from various sources as indicated except for the F results of the four samples from the Pamukkale group which were taken from Simsek (1982). The sampling dates for the Li analyses are not known, except for the Pamukkale group which was collected from MTA. Time variations of the Li concentrations in the Kizildere well waters are very small, so the Li concentrations of samples taken at any time can be taken to be representative. The sampling date for isotopic analysis in Table 3 is February 15, 1979.

Almost all the wells and springs of high temperature and boiling springs are located in the Kizildere and Tekkehamam areas. Their temperatures are in the range of 55.5-100°C. The flowrate of Demirtaş spring decreased after the plant started production, and sometimes it dries up. All water from both wells and springs in these areas are of the Na-SO<sub>4</sub>-HCO<sub>3</sub> type.

The temperature of the water in the Buldan area, which is located in Gediz graben, ranges from 36°C to 56.8°C. The temperature of Kamara spring has decreased from 57 to 32°C in the last 22 years. A well was drilled to 145 m depth in the area in early 1998 and discharged 4 l/s of water at 55°C. The hotels in the area were built for health spa purpose. The Yenice, Kamara, and Bolmekaya waters can be classified as Ca-HCO<sub>3</sub>, Na-HCO<sub>3</sub> and Mg-HCO<sub>3</sub> types, respectively.

In the Pamukkale area there are about 17 warm spring discharges. Only three of them have high flowrate with a total flow of more than 350 l/s at 35.5°C. These waters are of the Ca-Mg-HCO<sub>3</sub>-SO<sub>4</sub> type, and deposit white travertine. In the Karahayit area the Kizilleğen hot spring is the main thermal spring feature. It has almost the same composition as the Pamukkale water. At present, there are more than 100 wells in the town of Karahayit, in an area of less than 4 km<sup>2</sup>. These shallow wells were drilled for commercial purposes such as swimming pools, health spas and hotels during the last few decades. The temperature of the spring water has decreased from 54.4 to 42°C as well as the integrated discharge in the last six years, due to over-exploitation from the wells.

The waters from the Kizildere wells and the waste water is similar, naturally. The dominant cation is Na while the dominant anions are HCO<sub>3</sub> and SO<sub>4</sub>. The chemical composition of the hot spring discharges (samples 1 and 2) is quite close to Kizildere well water. However, the wells are higher in silica, slightly higher in chloride but lower in magnesium. The Tekkehamam thermal waters are lower in Na, K and Cl than the Kizildere water, generally lower in SiO<sub>2</sub> and B but higher in Ca, Mg and SO<sub>4</sub> and similar in total carbonate (Table 3). Water from other areas shows greater differences but follows the same general pattern, but tend to be higher in dissolved carbonate carbon.

The ionic balances of the water analyses were calculated by the WATCH programme (Arnórsson et al., 1982). Ionic balance gives information regarding the quality of the analysis, at least for those ions which occur in the highest concentrations. As can be seen from Table 3, ionic balance of the waters varies between -70.8 and 0.52% indicating that some of the analyses are not of acceptable quality. The tritium and deuterium contents of the water from all the areas are almost the same, whereas δ<sup>18</sup>O values decrease (become more negative) from the Kizildere group to Pamukkale and eastwards.

The gas/steam ratios for Kizildere wells are shown in Table 4. All wells have similar aquifer temperature and liquid enthalpy. At the wellhead separator pressure of about 4 bars abs, the wells produce about 18% steam (by weight) and 82% water. Gas/steam ratios and %CO<sub>2</sub> are higher in KD-6 and KD-13 than in other wells. In the Kizildere wells, the gas consists almost entirely of CO<sub>2</sub> (Table 5). N<sub>2</sub> is very high in well KD-14 but that is thought to be due to atmospheric contamination of the sample.

TABLE 4: Gas/steam ratio measurements for Kizildere wells (from ENEL et al., 1989)

Well No.	Date	G/S (NI/kg)	% CO <sub>2</sub>	Conden. V. cc	P <sub>atm</sub> (mm Hg)	T <sub>gas</sub> (°C)	WHP (kg/cm <sup>2</sup> )	P <sub>sep</sub> (kg/cm <sup>2</sup> )	T <sub>sep</sub> (°C)	Q <sub>w</sub> (t/h)	Q <sub>tot</sub> (t/h)
KD-6	25.04.1988	115.0	18.3	86-86	747.2	18.6	16.0	4.15	148	106	130.0
	26.04.1988	113.4	18.1	87-88	747.8	19.0	16.0	4.20	148	106	130.0
	27.04.1988	114.5	18.2	86-87	745.4	18.4	16.8	4.12	148	106	130.0
	02.05.1988	102.0	16.8	96-98	747.0	17.4	16.5	4.05	146	106	130.0
	03.05.1988	101.0	16.6	99-99	750.4	17.6	16.2	4.50	147	106	130.0
	05.05.1988	100.8	16.0	104-107	751.2	18.2	16.2	4.40	149	106	130.0
	08.05.1988	94.6	16.5	98-97	749.8	21.0	16.1	3.85	145	106	130.0
	06.06.1988	114.0	18.0	84-84	742.2	24.4	16.5	3.80	146	106	130.6
	08.06.1988	114.0	18.3	85-82	744.8	26.0	16.9	3.70	-	106	130.6
	15.06.1988	117.7	18.8	80-82	745.5	26.0	26.0	3.80	146	81	99.3
	22.06.1988	110.0	18.2	85-84	743.6	30.0	30.0	3.65	145	148.3	182.4
KD-7	08.05.1988	66.6	11.6	146-145	749.8	22.8	14.8	3.74	145	-	-
	13.06.1988	68.5	11.8	138-134	743.8	29.0	15.0	3.90	147	52.5	64.6
KD-13	25.04.1988	99.4	16.3	102-100	745.4	15.2	17.2	3.82	150	-	-
	25.04.1988	96.1	16.0	103-97	744.8	24.0	16.6	3.90	-	140	173
	25.04.1988	100.2	16.5	96-93	745.5	27.0	16.5	3.90	149	119.6	147.1
	25.04.1988	95.7	16.2	96-98	743.6	30.0	16.6	3.80	150	105	129
KD-14	25.04.1988	73.2	12.6	136-138	745.4	14.8	16.0	3.95	147	-	-
	25.04.1988	70	12.1	136-134	743.8	27.0	15.5	4.00	150	148.3	182.4
KD-15	25.04.1988	73	12.5	137-137	745.4	15.4	15.1	3.90	149	-	-
	25.04.1988	70.8	12.2	138-135	744.2	22.0	15.0	4.05	157.5	119	147
	25.04.1988	72	12.4	130-132	743.8	26.6	15.1	3.90	150	108.7	133.8
	25.04.1988	68.5	11.8	136-140	742.6	26.0	15.0	3.87	149	106	130.5
KD-16	25.04.1988	71.3	12.3	141-141	745.4	14.2	16.0	3.90	152	-	-
	25.04.1988	69.7	12.0	140-138	744.2	21.5	16.0	3.90	152	211	260
	25.04.1988	67	11.7	139-143	743.8	26.0	16.0	3.94	153	203	250
	25.04.1988	117.7	18.2	140-140	742.6	25.0	16.5	3.88	151	208	255.9
KD-20	25.04.1988	80.7	13.7	125-122	745.4	16.4	17.0	3.95	156	-	-
KD-21	25.04.1988	74.2	13.6	135-135	745.4	15.0	16.0	3.94	150	-	-
	25.04.1988	73.1	12.6	130-130	746.0	26.0	15.0	4.00	-	156	191
	25.04.1988	73.5	12.6	125-130	742.4	27.6	16.7	3.70	-	61.0	75.0
	25.04.1988	67.7	11.7	141-141	745.9	25.0	15.0	3.80	150	171	210
KD-22	25.04.1988	74.2	12.7	130-132	749.8	22.6	16.0	3.80	146	-	-

G/S: gas/steam ratios (litre gas per kg steam at 25°C and 1 bar); % CO<sub>2</sub> in steam by weight

TABLE 5: Gas analysis for Kizildere wells (from ENEL et al., 1989)

Well no	Sampling date	H <sub>2</sub> (% vol.)	O <sub>2</sub> +Ar (% vol.)	N <sub>2</sub> (% vol.)	CH <sub>4</sub> (% vol.)	CO <sub>2</sub> (% vol.)	H <sub>2</sub> S (% vol.)	He (ppm)
KD-6	09.05.1988	0.3	0.1	1.8	0.3	97.5	<0.1	5.4
KD-6	15.06.1988	<0.1	2.7	11.8	<0.1	85.5	<0.1	5.9
KD-6	06.06.1988	<0.1	2.1	8.5	<0.1	89.4	<0.1	8.2
KD-7	08.05.1988	<0.1	0.1	0.5	0.1	99.3	<0.1	15.6
KD-7	29.06.1988	<0.1	2.4	8.8	<0.1	88.8	<0.1	7.7
KD-14	30.06.1988	<0.1	11.6	42.6	<0.1	45.8	0.1	11.6
KD-16	29.06.1988	<0.1	2.4	9.2	<0.1	88.4	<0.1	10.9
KD-21	23.06.1988	<0.1	1.6	3.6	<0.1	94.8	<0.1	14
KD-22	08.05.1988	<0.1	0.6	1.7	0.1	97.5	<0.1	15

## 4. METHODS

### 4.1 Calculation of total carbonate

Alkalinity is frequently determined instead of total carbonate and this is the case with the data included in this study. The reported  $\text{HCO}_3$  values taken from the present data, were converted to total carbonate carbon as  $\text{CO}_2$  (by assuming that alkalinity represents titration of the sample with acid from the reported pH to a pH of 4.5), correcting theoretically for interference from  $\text{SiO}_2$ , B and  $\text{H}_2\text{S}$  and liquid water. Details of the procedure are given in Appendix I.

### 4.2 WATCH program

The WATCH computer program (Arnórsson et al., 1982; Bjarnason, 1994) is a useful tool for interpreting the chemical composition of geothermal fluids. The WATCH program computes major aqueous species concentrations, activity coefficients, gas pressures, ionic balance, activity products (Q), and solubility products (K) of 29 selected geothermal minerals. Reference temperature for the speciation calculations can be chosen in several ways, i.e. measured temperature of well or spring, discharges or a geothermometry temperature or in fact by any arbitrary value. The geothermometry temperatures are retrieved from the activities of the chemical species.

The WATCH program can also be used to compute aqueous speciation and mineral saturation of water of a given composition when they change temperature conductively or boil adiabatically. The WATCH program was applied in the present study to obtain the following information:

1. Subsurface temperature (quartz geothermometer).
2. The calcium concentrations of the aquifer waters of the Kizildere wells at calcite saturation, both at the quartz temperature and at the measured aquifer temperature.
3. Determination of the state of mineral saturation upon adiabatic boiling of the aquifer water at Kizildere.
4. Determination of the state of mineral saturation in spring water.

### 4.3 Origin of the fluid

#### 4.3.1 Stable isotope composition

Deuterium and oxygen-18 are the most important natural isotopes of water. Deuterium is used as a natural tracer to locate the catchment area of a geothermal reservoir and to investigate the regional groundwater flow paths, while  $^{18}\text{O}$  shift for each system gives information about water-rock interaction at depth. The mean annual hydrogen and oxygen isotopic composition of precipitation in any area is related to the local mean annual temperature: the lower the temperature, the lower the content of heavy isotopes. The relationship between  $\delta D$  and  $\delta^{18}\text{O}$  is given by:

$$\delta D = 8 \delta^{18}\text{O} + B$$

where the constant  $B$  (the deuterium excess) is in most cases near 10. Its value, however, depends on climatic conditions being lower in a wet climate but higher in a dry climate. For the study areas which are located in the Mediterranean region, the value of the deuterium excess was taken to be 22.

#### 4.3.2 The Cl-SO<sub>4</sub>-HCO<sub>3</sub> diagram

This diagram, which was described by Giggenbach (1991), is used to classify geothermal fluids on the basis of the major anions, i.e. Cl, SO<sub>4</sub>, and HCO<sub>3</sub>. It also allows an immediate eyeball statistical

evaluation of groupings and trends. There are several typical groups of thermal waters such as volcanic and steam-heated water formed by the absorption of high temperature HCl containing volcanic emanations, or lower temperature H<sub>2</sub>S containing geothermal vapours, into groundwater. Most chemical geothermometers are not suitable for application to these generally quite acid waters, whereas they are suitable for neutral, low sulphate, high chloride geothermal waters along the Cl-HCO<sub>3</sub> axis, especially close to the Cl corner. The diagram may provide an initial indication of the mixing relationship or geographical groupings, with Cl waters forming a central core grading into HCO<sub>3</sub> waters towards the margins of a thermal area. The degree of separation between data points for high chloride and bicarbonate waters gives an idea of the relative degree of interaction of CO<sub>2</sub> charged fluids at lower temperatures, and of the HCO<sub>3</sub> contents increasing with time and distance travelled underground.

#### 4.3.3 The Cl-Li-B diagram

This diagram is useful for evaluating the origin of geothermal fluids. Among rock derived constituents lithium is least affected by secondary processes, so it can be used as a tracer for deep rock dissolution and as a reference for evaluating the possible origin of the main two conservative constituents of thermal waters, Cl and B. Once added, Li remains largely in solution. It is, however, striking that both Cl and B are added to the Li containing solutions in proportions close to those in crustal rocks. At high temperatures Cl occurs largely as HCl and B as H<sub>3</sub>BO<sub>3</sub>. Both are volatile and can be mobilized by high-temperature steam. At lower temperatures the acidity of HCl increases rapidly, and it is soon converted by reaction with the rock to less volatile NaCl; B remains in its volatile form to be carried in the vapour phase even at lower temperature. The B content of thermal fluids probably reflects, to some degree, the maturity of a geothermal system. Due to its volatility, B is likely to escape during the early heating up stages. Fluids from older hydrothermal systems can be expected to be depleted in the element.

#### 4.4 Geothermometers

The temperature of hot-spring water discharged at the surface and of hot water from shallow wells is generally lower than that of the deeper geothermal reservoirs. The main reason for cooling in upflow zones is conductive heat loss, boiling and mixing with colder waters.

Estimation of temperature at depth in geothermal systems is one of the most important tasks in geothermal exploration. Various geothermometers have been developed for this purpose including aqueous and gaseous species and isotopes as well as mixing models. These geothermometers use data on the chemical and isotopic composition of discharges from springs and shallow drillholes. These geothermometers are quantitative. Qualitative geothermometers have also been developed. They are based on the distribution and relative concentrations of volatile elements in waters and soils and variations in soil-gas compositions. The qualitative technique aims at locating anomalous concentrations of the indicator elements, in soils, soil gases, fumaroles, springs, streams and deposits from geothermal fluids. After measuring Hg in soil gas and in soil, and CO<sub>2</sub> in soil gas, preparation of iso-mercury and iso-carbon dioxide maps can aid the identification of geothermal anomalies. Mercury measurements in cores from shallow boreholes may give valuable information regarding reservoir temperature at depth. White (1970) reviewed the qualitative geothermometers that had been suggested up to 1970. Tonani (1970) suggested that enrichment of B, NH<sub>4</sub>, HCO<sub>3</sub>, Hg and H<sub>2</sub>S in near surface water may result from boiling at depth. High concentrations of volatile components often accumulate above or around a relatively shallow heat source. High H<sub>2</sub>S in water may indicate higher temperature at depth. Often high concentrations of Na, K, Cl, Li, Rb, Cs and As in geothermal waters are an indication of high temperatures. Mahon (1970) noted that high Cl/F and Cl/SO<sub>4</sub> ratios in water indicate generally high reservoir temperature. High Cl/(CO<sub>3</sub>+HCO<sub>3</sub>) and low Mg and Mg/Ca ratios are also indicative of high temperature. At high temperature, magnesium is effectively incorporated into clay minerals such as chlorite and montmorillonite, causing its aqueous concentration to be very low. Travertine deposition from hot-spring water has been considered an indication of low temperature (about 100°C).

Quantitative geothermometers can be divided into two groups, chemical and isotopic ones. The isotopic geothermometers are generally used for high-temperature water. The chemical geothermometers are based on temperature-dependent variations in the solubility of individual minerals and temperature-dependent exchange reactions which fix ratios of certain dissolved constituents. They are sustained by the evidence of chemical equilibria between deep solutions and different mineral phases. The silica geothermometers were developed by Fournier and Rowe (1966), Arnórsson (1975), Fournier and Potter (1982), Arnórsson et al. (1983) and Arnórsson (1985); the Na-K geothermometer by Fournier (1979), Arnórsson et al. (1983), Arnórsson (1985) and Giggenbach (1988); the Na-K-Ca geothermometer by Fournier and Truesdell (1973); and the K-Mg geothermometer by Giggenbach et al. (1983). All have been widely used to estimate subsurface temperatures in geothermal systems on the basis of the chemical composition of water collected from hot springs and shallow wells. The application is based on the following assumptions:

1. Temperature-dependent equilibrium is attained between the geothermal fluid and minerals in the host rock in the reservoir;
2. There are no changes in the composition of hot water in the upflow where cooling may occur and mixing with colder water does not.

The various chemical geothermometry equations used in the present study are shown in Appendix II. The different chemical geothermometers, when applied to the same water from springs or wells, may give quite different results due to a lack of equilibrium between the respective species and hydrothermal minerals or mixing with colder waters in the upflow. The principles of the chemical geothermometers applied in this study are discussed below.

#### 4.4.1 Silica geothermometers

The rates of dissolution and precipitation of quartz and amorphous silica change as logarithmic functions of absolute temperature, with moderately fast rates at very high temperatures and extremely slow rates at low temperatures (Rimstidt and Barnes, 1980). Geothermal waters attain saturation with quartz in geothermal reservoirs, at least if temperatures exceed 180°C. Equilibrium with chalcedony tends to be attained at lower temperatures. During cooling in upflow zones silica precipitation is generally limited, unless the water cools sufficiently to become amorphous silica supersaturated. Aqueous silica in excess of amorphous silica solubility may polymerize in solution rather than precipitate from it.

At temperatures of less than about 300°C, and at depths generally attained by commercial drilling into geothermal reservoirs, variations in pressure at hydrostatic conditions have little effect on the solubilities of quartz, chalcedony and amorphous silica (Fournier and Rowe, 1977).

The solubility of all silica minerals increases strongly with temperature up to about 300°C. The solubility of the silica minerals is affected by pH when above about 9. The ionic strength does not significantly affect the solubility of silica minerals because they equilibrate with an uncharged species,  $H_4SiO_4$ .

The quartz geothermometer gives higher reservoir temperature than the chalcedony geothermometer for the same concentration of silica due to the lower solubility of the former. In general, the quartz geothermometer is applied at temperatures higher than 180°C, and both the chalcedony and the quartz geothermometers at temperatures below 180°C. When the silica geothermometers are applied to mixed waters they yield low temperature estimates. Generally speaking, the quartz geothermometer yields reliable values at temperatures between 150 and 225°C.

#### 4.4.2 Cation geothermometers

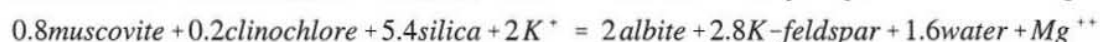
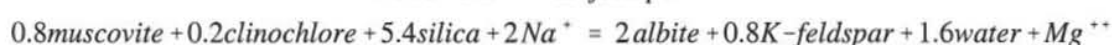
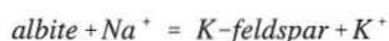
**The Na-K geothermometer** is based on simultaneous equilibrium between albite, K-feldspar and

solution. It appears to take longer time to come close to equilibrium with alkali feldspars than with either quartz or chalcedony. Therefore, there is a tendency to take the Na/K ratio to indicate temperatures at deeper levels in geothermal systems than the silica geothermometers.

Empirical calibration of the Na-K geothermometer has been proposed by various authors. They lie between the albite-microcline and albite-adularia curves ( $\log(\text{Na/K})$  versus  $1000/T$ ). The reliability of subsurface temperatures estimated by the Na-K geothermometer depends on the particular mineral assemblage and the structural states of the minerals with which the circulating water equilibrates. Fournier (1991) noted that the Na-K geothermometer tends to give high temperatures when applied to  $\text{NH}_4$ -rich waters, apparently due to a reaction with organic-rich sediments.

**The Na-K-Ca geothermometer**, which is entirely empirical, is based on exchange reactions of Na, K, and Ca with mineral solid solutions. When applied to Mg-rich waters, it gives very high temperatures. Fournier and Potter (1979) devised a Mg correction in order to overcome this problem (see Appendix II). Mg concentrations in geothermal fluids rapidly decrease with increasing temperature. Mg correction for water with low temperatures may be substantial. When applying a Mg correction to high-temperature water which has picked up Mg in the upflow tends to give low reservoir temperature estimates.

**The Na-K-Mg triangular diagram** proposed by Giggenbach (1988) is useful for distinguishing equilibrated from non-equilibrated water. By Giggenbach's classification, there are non-equilibrated waters which are separated as immature, partially equilibrated and fully equilibrated. The following three reactions seem to control the relative concentrations of Na, K and Mg, they are used to construct the triangular diagram:



The position of the full equilibrium curve depends on both the selected Na/K, and K/Mg geothermometer equations. The waters that plot between the full equilibrium and immature water curves, may result from mixing a fully or partly equilibrated water with cold immature water. Immature waters plot rather close to the Mg-corner. Application of cation geothermometers to estimate subsurface temperature is not reliable for such water.

**Solution-mineral equilibria:** Reed and Spycher (1984) indicated that the best solution to estimate reservoir temperature involves evaluation of the saturation state of a particular water composition with respect to selected minerals as a function of temperature. Saturation index, SI which is the degree of saturation of a particular mineral in an aqueous solution, can be obtained from its solubility product and its reaction quotient (activity product)

$$SI = \log Q - \log K = \log(Q/K)$$

where  $Q$  is the calculated activity product and  $K$  is the equilibrium constant.

The diagram of SI versus temperature depicts the equilibrium state of the fluid for each mineral as a function of temperature. The zero line (saturation line) in the SI diagram shows the equilibrium state with an aqueous solution for each mineral. Positive SI corresponds to supersaturation whereas negative values correspond to undersaturation. The point at which several minerals cross the zero line gives the most reliable estimate of underground temperature.

#### 4.5 Mixing models

The silica-enthalpy and the chlorine-enthalpy mixing models were applied to the water in this study to estimate subsurface temperature in the study areas.

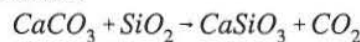


## 5. GEOCHEMICAL FEATURES OF THE WATERS

### 5.1 The Kizildere geothermal area

#### 5.1.1 Origin and type of water

**Isotopic composition of the water:**  $\delta D$ ,  $\delta^{18}O$  and tritium compositions were determined by Filiz (1982) in only 2 samples from wells KD-6 and KD-13. The  $\delta D$  values in these samples are about -54‰ and the  $\delta^{18}O$  values -6.03 and -5.53‰, respectively (Figure 6). The data points for KD-6 and KD-13 plot to the right of the meteoric line. In other words, they are far removed from the  $\delta D$ - $\delta^{18}O$  composition of meteoric water. This is known as an "oxygen shift" (Truesdell and Hulston, 1980) and is due to oxygen isotope exchange between the water and the reservoir rocks. Such a shift is most pronounced at high temperatures and at low water-rock ratios. Meteoric water is not in oxygen isotope equilibrium with rocks, the latter being much richer in  $^{18}O$ . Changes towards equilibrium involve an oxygen isotope exchange that causes the waters to become enriched in  $\delta^{18}O$  and the rocks correspondingly depleted. Filiz (1982) concluded that the origin of  $CO_2$  gas, discharged from the Kizildere wells, was from decomposition of calcereous rocks (metamorphism) at temperatures of at least 350°C. The process can be expressed in the following reaction:



The tritium content of these waters is 14-28 TU. It is concluded that the Kizildere reservoir water is local meteoric water by origin that is at least 50 years old. The observed oxygen shift is in line with the relatively high reservoir temperatures.

**The  $Cl-SO_4-HCO_3$  triangular diagram:** Chloride, which is a conservative constituent in geothermal fluids, does not take part in reactions with rocks after it has dissolved. Therefore, it can be used as a tracer in geothermal investigations. Chloride concentration in the water changes only upon mixing with water of different Cl content. In the triangular  $Cl-SO_4-HCO_3$  diagram, data points for waters from Kizildere wells plot in the  $HCO_3$  area, near the  $HCO_3$  corner (Figure 7). This area on the diagram represents peripheral water in many types of volcanic fields. But, this is not the case in the study area. High chloride, but low sulphate and bicarbonate water is typical for high temperature systems associated with andesitic and rhyolitic magmatism. However, the reservoir rocks in the Kizildere and the neighbouring geothermal areas are composed of limestone, intercalation of marble and schist, and quartzite. The water emerging from such a reservoir is naturally rich with calcium and bicarbonate ions as in the studied water. Some of this water contains relatively high concentrations of sulphate, the source of which may be oxidation of  $H_2S$  gas escaping from magma, and/or dissolution of minerals like gypsum and celestite ( $SrSO_4$ ).

Altunel (1996) concluded that the travertines in Pamukkale are about 400,000 years old. This is an indication that geothermal activity in the area has lasted for at least 400,000 years. The thermal water

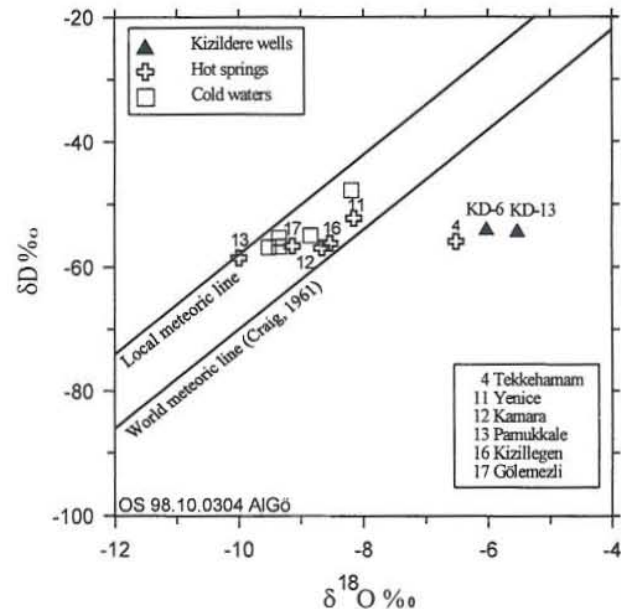


FIGURE 6:  $\delta D$  vs.  $\delta^{18}O$  for water in the study area

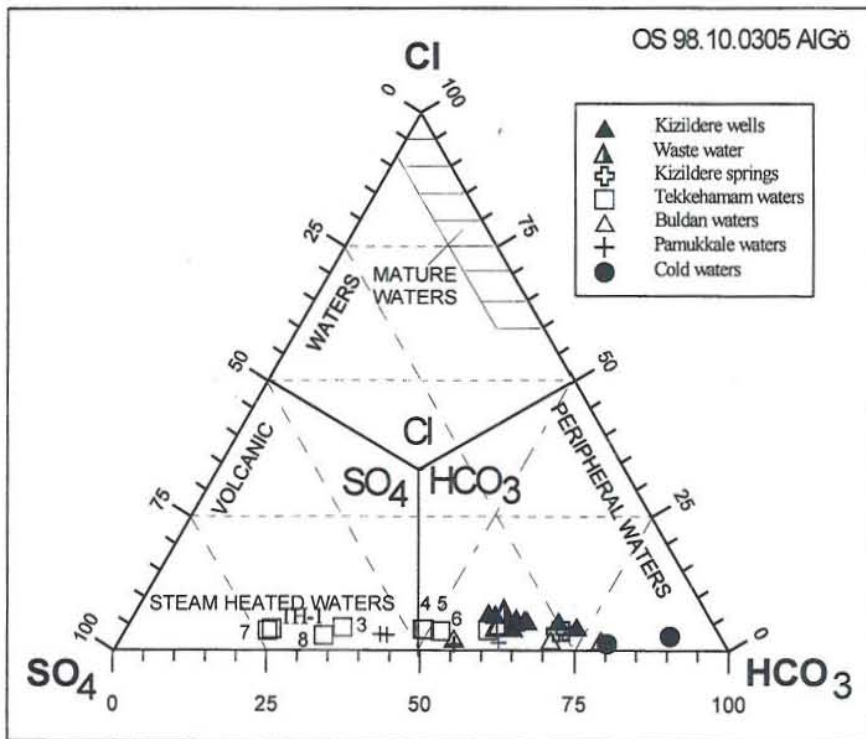


FIGURE 7: The Cl-SO<sub>4</sub>-HCO<sub>3</sub> diagram for the waters in the study area

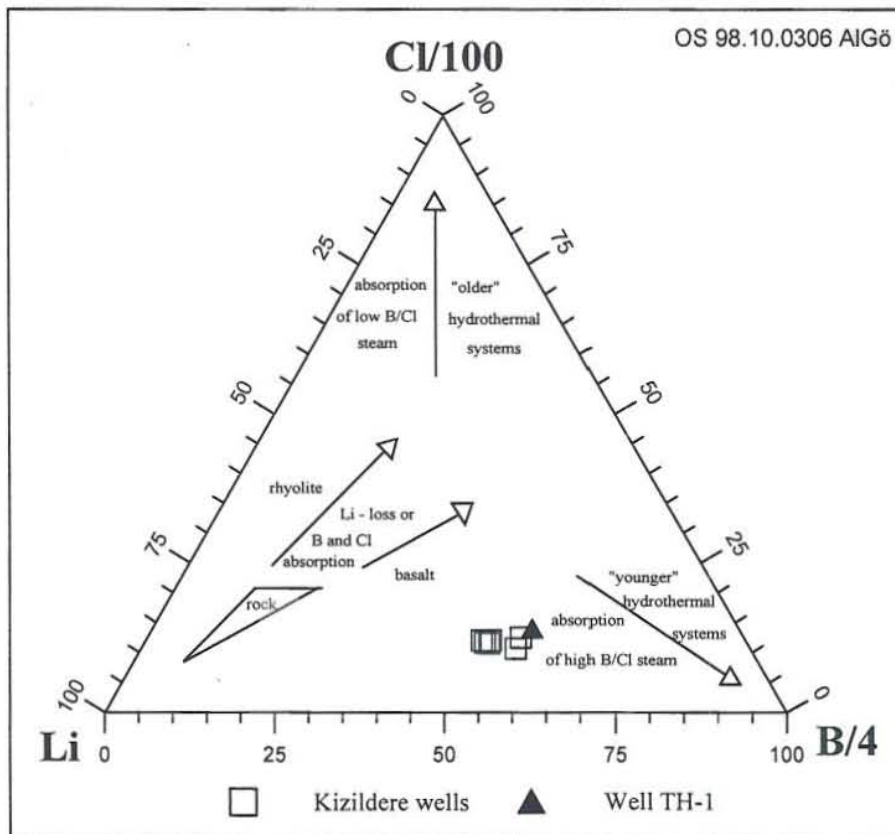


FIGURE 8: The Cl-Li-B diagram for the waters in the study area

of Kizildere was interpreted as old water with an age of 10,000 to 30,000 years by Özgür et al. (1998). As a result, it can be said that this triangular diagram, which was constructed for a definite type of system in specific rocks, i.e. andesite and rhyolite, cannot be applied to the waters of the study area.

**Cl-Li-B triangular diagram:** A plot of the relative concentrations of chloride, lithium and boron is shown in Figure 8. The well water at Kizildere and Tekkehamam plots near the Li-B tie line. In areas of andesitic and rhyolitic volcanism, mature geothermal water plots towards the Cl-corner of this diagram whereas water in young systems may plot near the boron corner due to the abundant supply of this element from degassing fresh magma. The relative distribution of Cl, B and Li in the well water from Kizildere and Tekkehamam is thought to reflect their abundance in the rocks with which the water has reacted rather than the maturity of the system.

**5.1.2 Estimation of subsurface temperature**

As mentioned earlier, there are three permeable horizons in the Kizildere geothermal area. They consist of (from the bottom), quartzitic gneiss with temperature of 242°C, alternation of marble-quartzite-schist

with 202°C and Pliocene limestones with 180°C. Measured aquifer temperature at sampling dates for producing wells at Kizildere varies between 196 and 211°C (Table 6). These values are 1-6°C lower than measured values during the initial tests of the wells.

TABLE 6: Results of different geothermometers for Kizildere wells  
(see Appendix II for equations)

No.	Tm	Quartz			Chalcedony		Na-K					Na-K-Ca	Na-K-Ca <sup>#</sup>
		1*	3	5	7	9	10	11	12	13	14	15	15
KD-6	196	208	204	204	194	187	182	213	190	228	178	248	209
KD-13	195	208	204	204	194	187	194	222	201	237	191	246	215
KD-14	207	212	209	209	200	192	196	224	203	238	193	251	230
KD-15	205	213	209	209	200	192	191	220	198	235	187	240	218
KD-16	211	213	210	210	202	193	194	222	201	237	190	240	231
KD-20	201	208	205	205	195	187	190	219	197	234	186	236	214
KD-21	202	212	208	208	199	191	187	216	194	231	183	244	216
KD-22	202	212	209	209	200	192	198	225	205	240	195	255	224
Mean	202	211	207	207	198	190	192	220	199	235	188	245	220

Tm: Measured temperature; \*: Calculated by WATCH program;

#: Using calculated Ca concentrations as the calcite saturation in the deep water

- |  |  |                                |
|--|--|--------------------------------|
| 1 Fournier and Potter (1982)               | 6 Fournier (1977), no steam loss           | 11 Fournier (1979)             |
| 2 Fournier (1973), no steam loss           | 7 Fournier (1977), max. steam loss         | 12 Arnórsson et al. (1983)     |
| 3 Fournier (1973), max. steam loss         | 8 Arnórsson et al. (1983), no steam loss   | 13 Giggenbach (1988)           |
| 4 Arnórsson et al. (1983), no steam loss   | 9 Arnórsson et al. (1983), max. steam loss | 14 Fournier & Truesdell (1973) |
| 5 Arnórsson et al. (1983), max. steam loss | 10 Truesdell (1976)                        | 15 Fournier (1973)             |

Four geothermometers, i.e. the quartz, chalcedony, Na-K and Na-K-Ca geothermometers were used in this study to estimate aquifer temperatures for the Kizildere wells. A total of 15 equations belonging to these four geothermometers were applied to water from Kizildere wells. The results are shown in Table 6 together with measured aquifer temperature. The third column in the table represents reservoir temperature calculated by the WATCH program using the quartz solubility curve of Fournier and Potter (1982).

The samples were collected from the weirbox. Thus, they have boiled from the aquifer pressure to atmospheric pressure. It is considered quite reasonable to assume the boiling to be adiabatic in the well. For this, quartz and chalcedony geothermometry equations which assume adiabatic boiling (maximum steam loss), are considered appropriate (Table 6).

The reservoir temperature calculated by the quartz geothermometry equations varies between 204 and 213°C. These values are very close to the measured aquifer temperatures which average 202°C. It is important to notice that the difference between quartz and measured temperatures is smallest for well KD-16, which has a highest measured temperature of 211°C, only 1-2°C, whereas for well KD-13, which has the lowest measured temperature of 195°C, the difference is 9-13°C. For this geothermometer, deviation from the average of measured aquifer temperatures is +13 to -1°C. The chalcedony geothermometry equations give 2 to 18°C lower values than the measured temperature. It appears that the water tends to equilibrate with quartz rather than chalcedony. As can be seen from Table 7, the difference between the quartz equilibrium and measured aquifer temperatures increases with decreasing measured temperatures.

TABLE 7: Differences between measured aquifer temperatures and geothermometry temperatures for Kizildere wells (see Appendix II for equations)

No.	Tm	Quartz		Chalcedony			Na-K						Na-K-Ca	Na-K-Ca <sup>#</sup>
		1*	3 / 5	7	9	M	10	11	12	13	14	M		
KD-6	196	12	8	-2	-9	-5.5	-14	17	-6	32	-18	2	52	13
KD-13	195	13	9	-2	-10	-6	-1	27	6	42	-4	14	51	20
KD-14	207	5	2	-7	-15	-11	-11	17	-4	31	-14	4	44	23
KD-15	205	8	4	-5	-13	-9	-14	15	-7	30	-18	1	35	13
KD-16	211	2	-1	-9	-18	-13.5	-17	11	-10	26	-21	-2	29	20
KD-20	201	7	4	-6	-14	-10	-11	18	-4	33	-15	4	35	13
KD-21	202	10	6	-3	-11	-7	-15	14	-8	29	-19	0	42	14
KD-22	202	10	7	-2	-10	-6	-4	23	3	38	-7	11	53	22
Mean	202	8	5	-4	-12	-8	-10	18	-3	33	-14	4	43	18

Na-K geothermometry temperatures vary between 182 and 240°C, depending on the choice of temperature equation. The average value from Arnórsson et al. (1983) Na-K geothermometry equation is very close to measured temperature values, the difference being only 3°C. The values calculated from Truesdell's (1976) equation are a little low, but not significantly. Temperatures calculated using other Na-K equations deviate significantly from the measured temperatures, that of Fournier and Truesdell (1973) giving low values but those of Fournier (1979) and Giggenbach (1988) giving high values. The average value of the five Na-K geothermometry equations is only 4°C higher than the average measured aquifer temperature, 1°C lower than the average quartz equilibrium temperature (Table 7). These results are taken to indicate that, water is close to equilibrium with alkali feldspars in the Kizildere reservoir.

The Na-K-Ca geothermometer yields the highest aquifer temperature estimates. They range between 236 and 255°C. These values are 29 to 53°C higher than those measured. The discrepancy is, to some extent, due to calcium loss from the water as it boils and deposits calcium carbonate. If corrected calcium values are used, which correspond to calcite saturation in the aquifer, Na-K-Ca temperatures become 9-39°C lower and 13-23°C higher than measured aquifer temperatures, the average difference being 18°C.

The geothermometry results for the Kizildere wells can be summarized as follows: For the Kizildere wells, the Na-K geothermometry equations giving the best match with measured aquifer temperature are those of Arnórsson et al. (1983) and Fournier and Truesdell (1973). The equations of Fournier (1979) and Giggenbach (1988) yield higher temperatures. The Na-K-Ca geothermometer also indicates higher temperatures. This is partly caused by calcium loss from the water during boiling through calcite precipitation. Part of the difference could be due to imprecise calibration or be an indication of higher temperatures at deeper levels. As a matter of fact, in well R-1 drilled to 2261 m depth, the bottom temperature was measured at 242°C. That value matches well the Na-K-Ca temperature. The water composition from this well can aid more reliable interpretation about estimation of reservoir temperatures in the Kizildere geothermal field.

The Na-K-Mg triangular diagram (Giggenbach, 1988) is shown in Figure 9. The equilibrium state of water from Kizildere wells was evaluated using the diagram. All water from Kizildere wells is located a little above the Arnórsson full equilibrium curve. The Na-K-Mg triangular diagram yields reservoir temperatures ranging between 190 and 210°C for this water.

### 5.1.3 Scaling

At Kizildere, calcite scaling in wells has caused operational problems. Large amounts of scale also form in the separators and in the waste water systems. The Kizildere geothermal reservoir is in single-liquid

phase. Depressurization, as the water ascends in boreholes during production, leads to boiling of the about 200°C reservoir water. The steam discharged at the surface contains 10-20% CO<sub>2</sub> (by weight). CO<sub>2</sub> degassing of the water as it boils causes an increase in pH and, as a result, an increase in the aqueous CO<sub>3</sub><sup>-2</sup> concentrations. Calcium concentrations also increase due to steam loss. These changes cause the water to become strongly calcite supersaturated,

producing calcite scaling. The pH of the aquifer water as calculated by WATCH at the quartz equilibrium temperature, varies from 5.51 for well KD-20 to 6.74 for KD-22 (Table 8). As can be seen from Table 9, the concentrations of all constituents in the reservoir water are lower than in the surface discharge except for CO<sub>2</sub> and Ca.

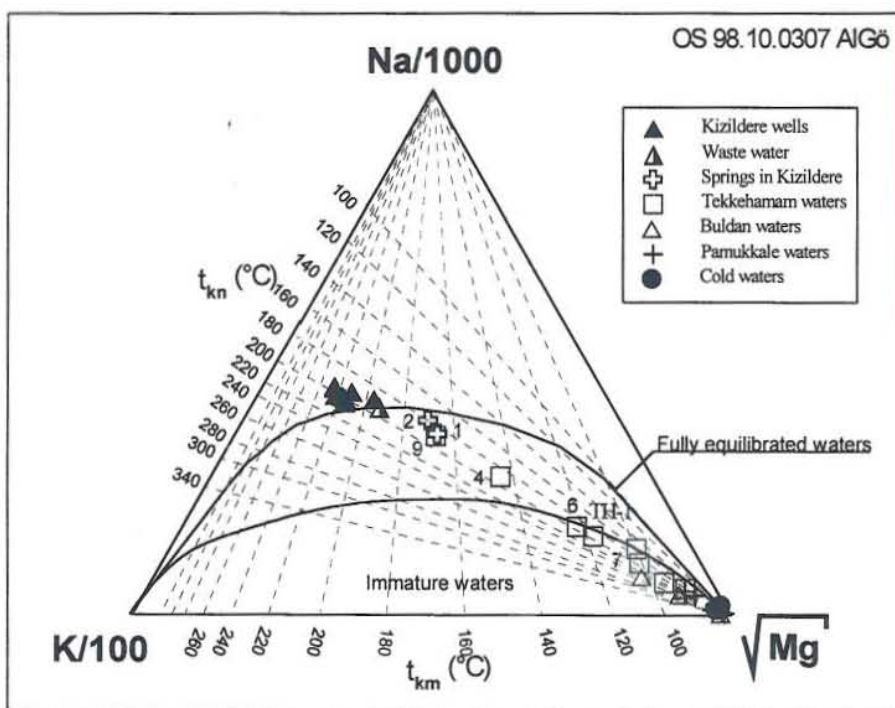


FIGURE 9: The Na-K-Mg diagram for the waters in the study area

TABLE 8: Gas partial pressures (bar-a) and depth of scales (m) in 1994 in some Kizildere wells (from MTA, unpublished results)

Well No.	KD-6	KD-7	KD-13	KD-14	KD-15	KD-16	KD-20	KD-21	KD-22
P <sub>CO2</sub>	57.7	48.0	54.5	21.5	57.3	48.2	24.1	31.5	26.8
P <sub>H2S</sub>	0.006	0.008	0.007	0.004	0.002	0.006	0.007	0.009	0.004
P <sub>NH3</sub>	0.0007	0.002	0.0007	0.002	0.001	0.002	0.002	0.002	0.002
P <sub>H2</sub>	0.004	0.003	0.004	0.0006	0.006	0.005	0.0005	0.001	0.0005
P <sub>O2+Ar</sub>	0.16	0.13	0.16	0.014	0.109	0.09	0.023	0.027	0.025
P <sub>CH4</sub>	1.2	0.97	1.13	0.92	1.08	0.895	0.112	0.184	0.123
P <sub>N2</sub>	1.84	1.43	1.72	0.15	1.56	1.28	0.18	0.291	0.199
P <sub>H2O</sub>	13.7	16.9	14.0	18.0	18.3	19.5	16.9	17.2	16.9
P gas tot.	74.6	67.5	71.5	39.7	63.8	69.9	41.3	49.2	44.1
Deepest scale level	640	-	590	510	460	560	490	550	558

According to Giese et al. (1998), the first level of boiling in well KD-22 is at 600 m below the wellhead and significant scale formation begins at a depth of 550 m. It is clear that degassing of the boiling water, with respect to CO<sub>2</sub>, leads to increased fluid flow velocities, increased water pH and precipitation of calcite. The scale thickness formed in one year and its depth, as measured by go-devil in wells KD-6, KD-7, KD-14, KD-15 and KD-16, are shown in Table 10 and Figure 10. Tan (1985) noted that if wellhead pressure is kept low, production is high but scale formation is also rapid. At a wellhead pressure of 15 kg/cm<sup>2</sup> g, a sharp decrease in the scaling rate is observed and this pressure value has been chosen as the optimum wellhead pressure of the wells in Kizildere geothermal area.

TABLE 9: Calculated composition of aquifer water at Kizildere

Well No.	T <sub>quartz</sub> (°C)	pH	Na	K	Ca	Mg	B (tot)	SiO <sub>2</sub>	CO <sub>2</sub> (tot)	Cl	SO <sub>4</sub>	F	Ionic bal. % diff.
KD-6	207.5	5.52	967	100	26.0	0.28	16.2	289	38022	98	444	14.1	20.66
KD-13	207.5	5.52	1031	109	28.5	0.18	21.0	289	35104	101	613	15.9	21.78
KD-14	212.3	5.90	1104	119	9.7	0.16	19.1	307	25450	113	577	19.4	0.84
KD-15	212.6	5.69	1049	108	19.5	0.12	19.3	307	25371	110	571	17.5	28.63
KD-16	213.3	6.02	1094	116	7.8	0.19	18.8	311	13047	106	558	18.4	30.38
KD-20	208.1	5.51	1089	111	30.5	0.12	19.1	291	28367	111	562	17.8	43.13
KD-21	211.5	5.65	1040	103	19.5	0.19	19.2	304	23858	110	557	16.5	35.48
KD-22	211.6	6.74	1001	110	15.0	0.19	19.6	308	3663	107	572	17.7	11.71

TABLE 10: Depths reached by the go-devils in wells during removal of scales; the first 9 columns of the table represent results from 1976-1977 (Tan, 1985), but the last 4 columns results obtained during 14.10.1986-28.02.1987 (taken from MTA)

Well No.	PCD (inch)	PT (months)	Go-devil depth (m)						PDAT (%)	WCD (m)	RBWD (m)	PAC (t/s)	WBP (kg/cm <sup>2</sup> )
			9"	8"	7"	6"	5"	4"					
KD-6	9	10	-	0	40	47	112	575	44	660	851	130	76.86
KD-7	6	12	-	-	-	0	16	123	66	597	667.5	145	60.41
KD-13	-	-	-	-	-	-	-	-	-	595	760	152	70.88
KD-14	9	10	0	453	453	-	-	-	18	410	525	54	48.80
KD-15	9	12	-	0	3	50	377	-	47	385	502	60	46.13
KD-16	11	18	0	40	80	124	157	190	74	490	660	63	59.63
KD-20	-	-	-	-	-	-	-	-	-	455	730	245	65.26
KD-21	-	-	-	-	-	-	-	-	-	510	-	250	79.89
KD-22	-	-	-	-	-	-	-	-	-	560	-	313	80.70

PCD: Production casing diameter; PT: Production time; WCD: Depth to which well was cleaned; PDAT: Decrease in production between two cleaning operations; RBWD: The deepest level of scale; PAC: Production after cleaning; WBP: Bottom well pressure.

Analysis of scales from wells at Kizildere made by MTA yielded the following results (Yildirim et al., 1997):

70-78% CaCO<sub>3</sub>, 18-20% SrCO<sub>3</sub>, 0.15-1.8% MgCO<sub>3</sub>, 0.2-5% SiO<sub>2</sub> (with traces of Al, Ba, Na, and Fe)

Mineralogical investigations made by Giese et al. (1998) for well KD-22 showed that scaling at depths between 550 m and 200 m contains nearly 90% calcite and 10% aragonite but in the upper part of the well the amount of aragonite increases to nearly 70%. The increase of aragonite in the scale in the upper part of the well has been correlated with increasing fluid velocity (Giese et al., 1998).

Figure 11 represents log (Q/K) (saturation index) versus temperature diagram for calcite, anhydrite, fluorite, amorphous silica, chalcedony and quartz for adiabatic boiling of Kizildere wells which were retrieved with the aid of WATCH. The analysed calcium concentrations in the surface discharge were increased to a level where the aquifer water was calculated to be calcite-saturated at both quartz equilibrium and measured aquifer temperature. Generally, the water is close to equilibrium with quartz, fluorite, and anhydrite in the aquifer and a little undersaturated with chalcedony and substantially so with amorphous silica.

According to the diagrams in Figure 11, boiling leads to sharp supersaturation with respect to calcite. The water also becomes supersaturated with quartz and chalcedony and generally with amorphous silica around 100°C. On the other hand, boiling and cooling causes the water to become progressively more undersaturated with anhydrite. Some of the well waters become fluorite-supersaturated upon boiling but others do not. Lándal and Kristmannsdóttir (1989) carried out scaling and corrosion tests on the Kizildere well water and they noted that these tests indicate a strong and rapid precipitation of calcium carbonate just after the water is discharged from the separator and much less after that. Yildirim et al. (1997) noted that after separation of liquid and vapour in the separators, and then in the weirboxes, the waste water calculated to be undersaturated with calcite below about 50-100°C, except for KD-16 which is still supersaturated at 50°C. As can be seen from Figure 11 all the well water at Kizildere calculated to be strongly calcite supersaturated at low temperatures. The cause of the

apparent discrepancy is that Figure 11 is based on calculated calcium concentrations to match calcite saturation in the aquifer but not actual calcium concentrations. The difference between the two concentrations is a measure of calcium lost from solution by calcite deposition.

Figure 12 shows calculated Ca concentrations at calcite saturation for both quartz equilibrium and measured aquifer temperatures for Kizildere wells. Figure 13 depicts how pH and aqueous concentrations of  $\text{Ca}^{+2}$ ,  $\text{HCO}_3^-$  and  $\text{CO}_3^{-2}$  change as water from well KD-6 boils adiabatically. Figure 14 shows the same for the activity and the activity coefficient as well as changes in  $\text{CO}_2$  concentrations. It is seen that pH increases drastically during the early stages of boiling and thereafter more gently. The cause is the sharp decline in the  $\text{CO}_2$  content of the water as it boils. The pH increase leads to an increase in the concentration of the  $\text{CO}_3$  ion by almost three orders of magnitude. Calcium concentrations increase by a factor of 5. This is due to steam loss only to a small extent. In the aquifer water, most of the calcium occurs as the  $\text{CaHCO}_3^+$  ion pair breaks down to release free  $\text{Ca}^{+2}$ . It is this disintegration of the  $\text{CaHCO}_3^+$  ion pair that is mostly responsible for the increased concentrations of  $\text{Ca}^{+2}$ . The increase in  $\text{Ca}^{+2}$ , and, in particular in  $\text{CO}_3^{-2}$ , is the cause of calcite supersaturation, created by the boiling process.

Calcite scale formation in wells at Kizildere causes production from individual wells to decrease by as much as 74% in one year. To cope with the scaling problem in the Kizildere well, chemical inhibitors and mechanical cleaning have been used. Phosponates have been injected at levels of 50-70 m below the flashing depth. This prevented scale formation (Mertoğlu et al., 1993). However, the injection has been discontinued due to the high cost of the chemicals and the breakdown of injection pipes due to vibration (Durak et al., 1993). At present, Kizildere wells are cleaned mechanically by RCHP (Rotating head

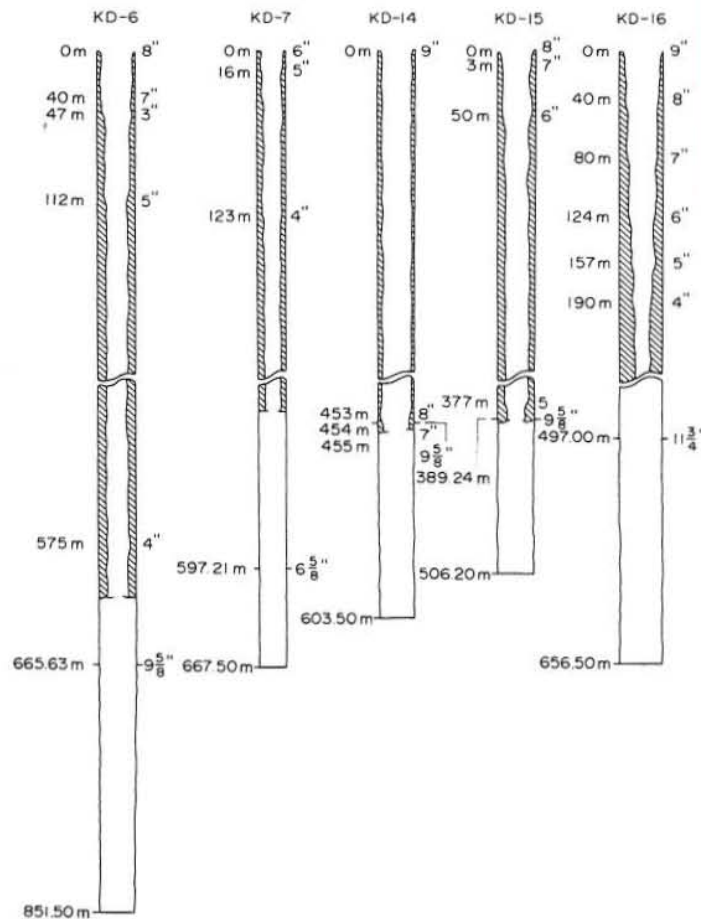


FIGURE 10: Scaling thickness measured by go-devil in wells after one year of production (from Tan, 1985)

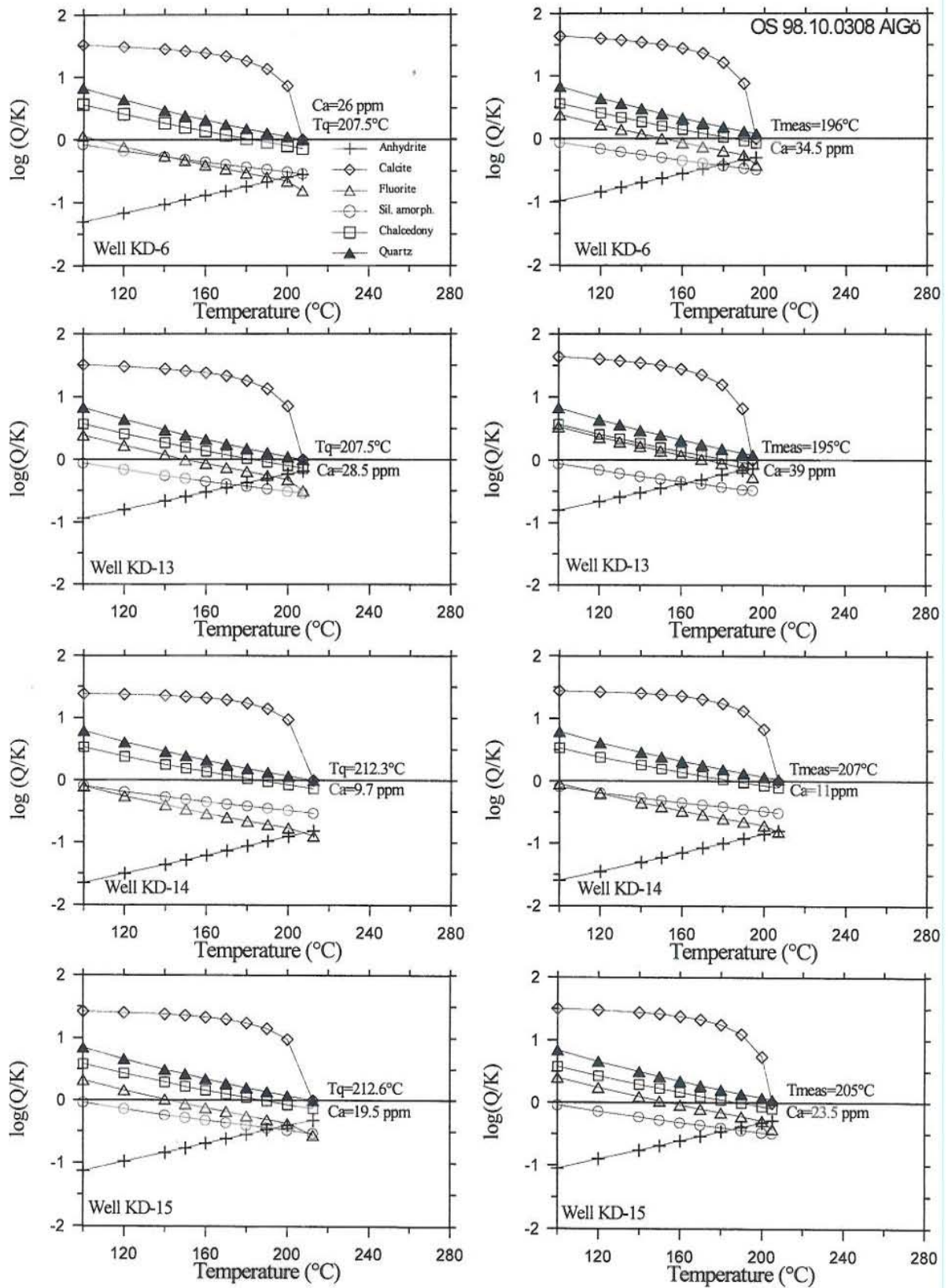


FIGURE 11: Mineral saturation diagrams for Kizildere well water during one step adiabatic boiling



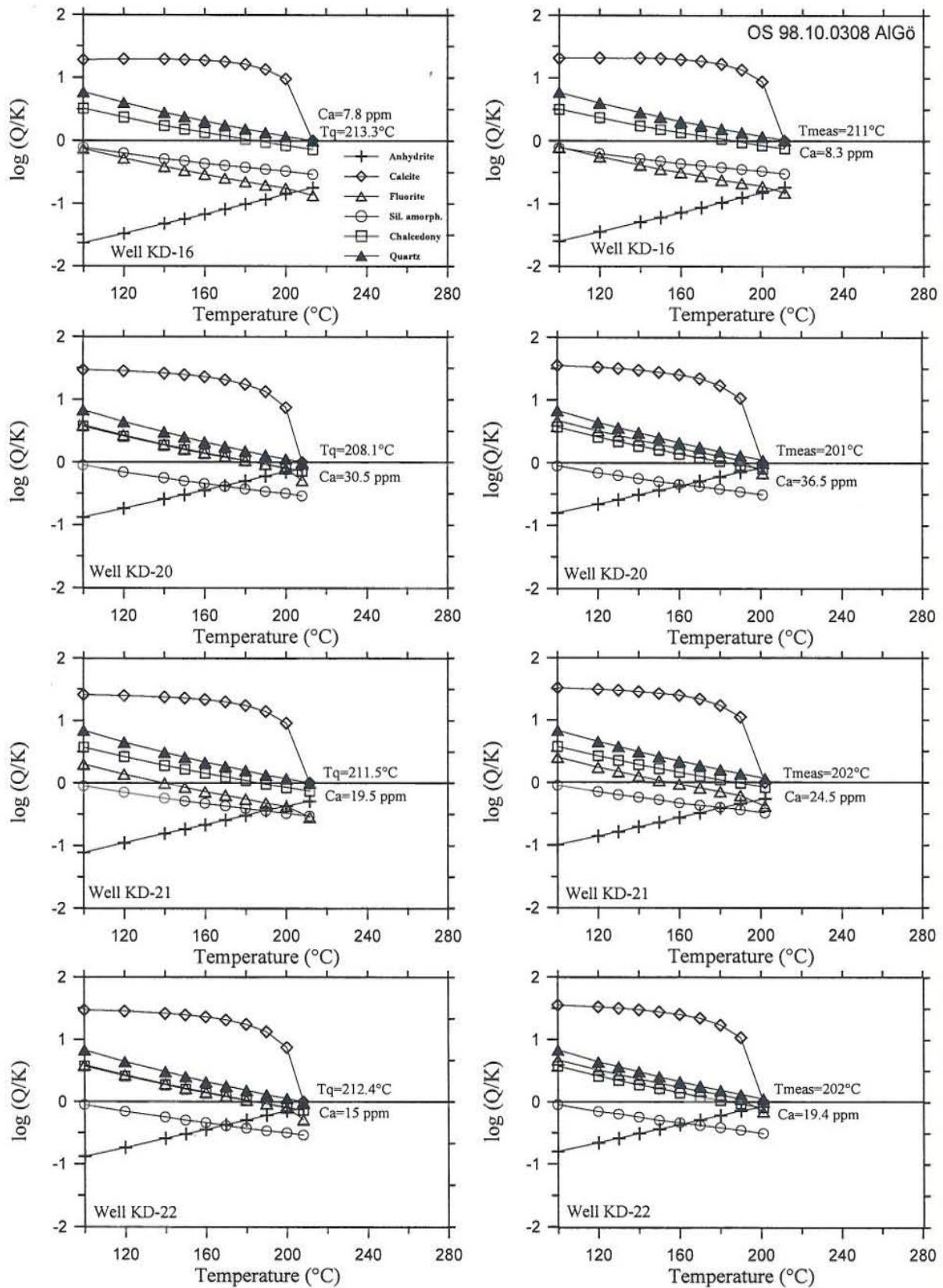
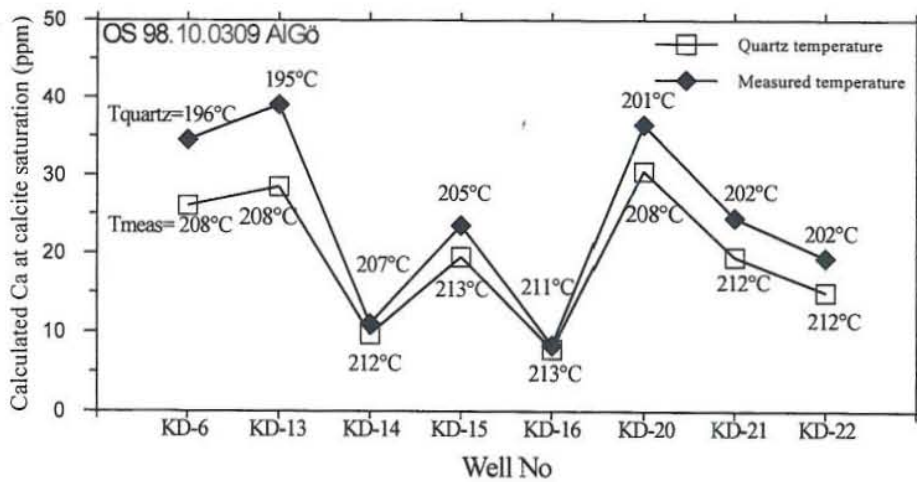


FIGURE 11: Continued



control preventer) two times a year. The montage, cleaning and de-montage processes are completed in fifteen days. The wellhead pressures are kept high in order to reduce the rate of scale formation, causing a decrease in electricity production to about 50% of installed capacity.

FIGURE 12: Calculated Ca concentrations at calcite saturations at quartz equilibrium and measured aquifer temperature for Kizildere wells

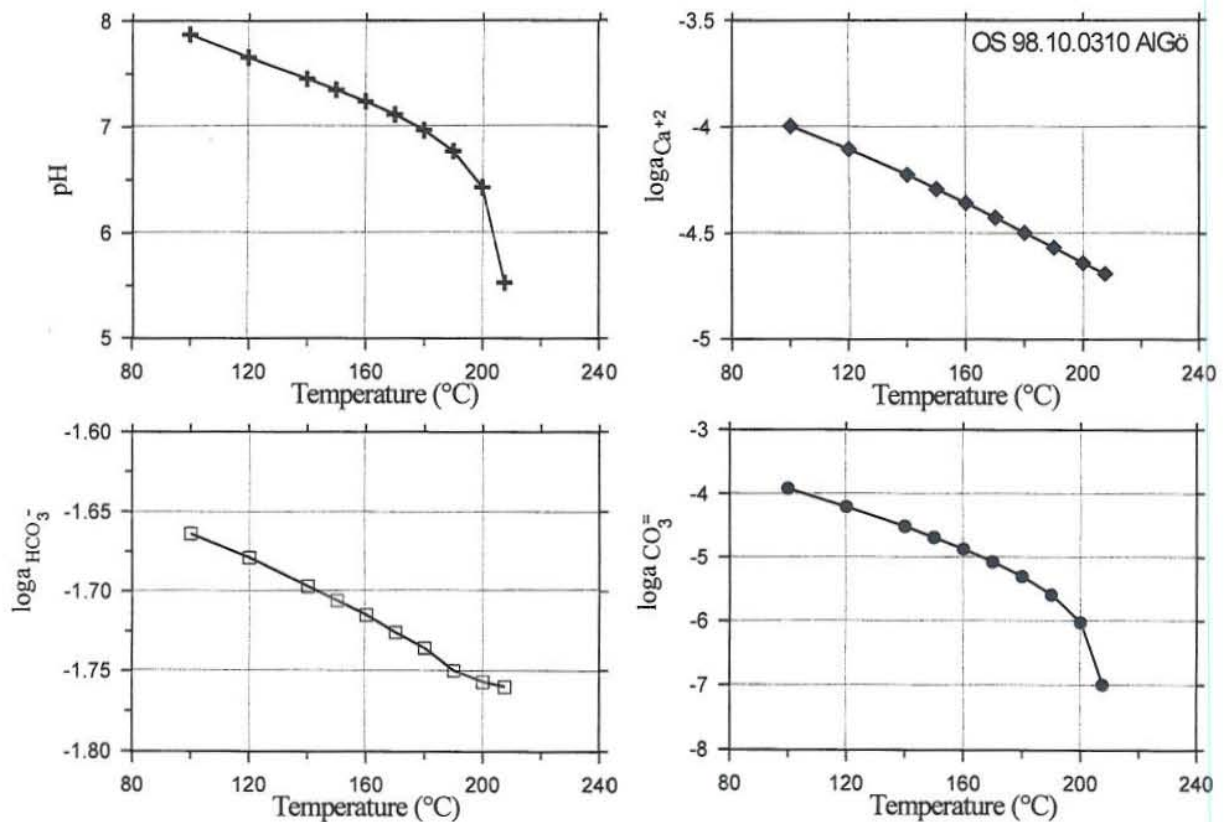


FIGURE 13: Changes in calcite saturation, pH and the activities (moles/kg) of calcium, bicarbonate and carbonate ions during one step adiabatic boiling of water for well KD-6

## 5.2 Other geothermal fields

### 5.2.1 Origin of the waters

**Isotopic composition of the water:** Figure 6 shows that the variation in  $\delta D$  is very small for water from all the study areas, the range being  $-52.2$  to  $-58.5\%$  (including Kizildere water). This is taken to indicate a common origin for all the water. The recharge area is likely to be at high elevation. Water from the

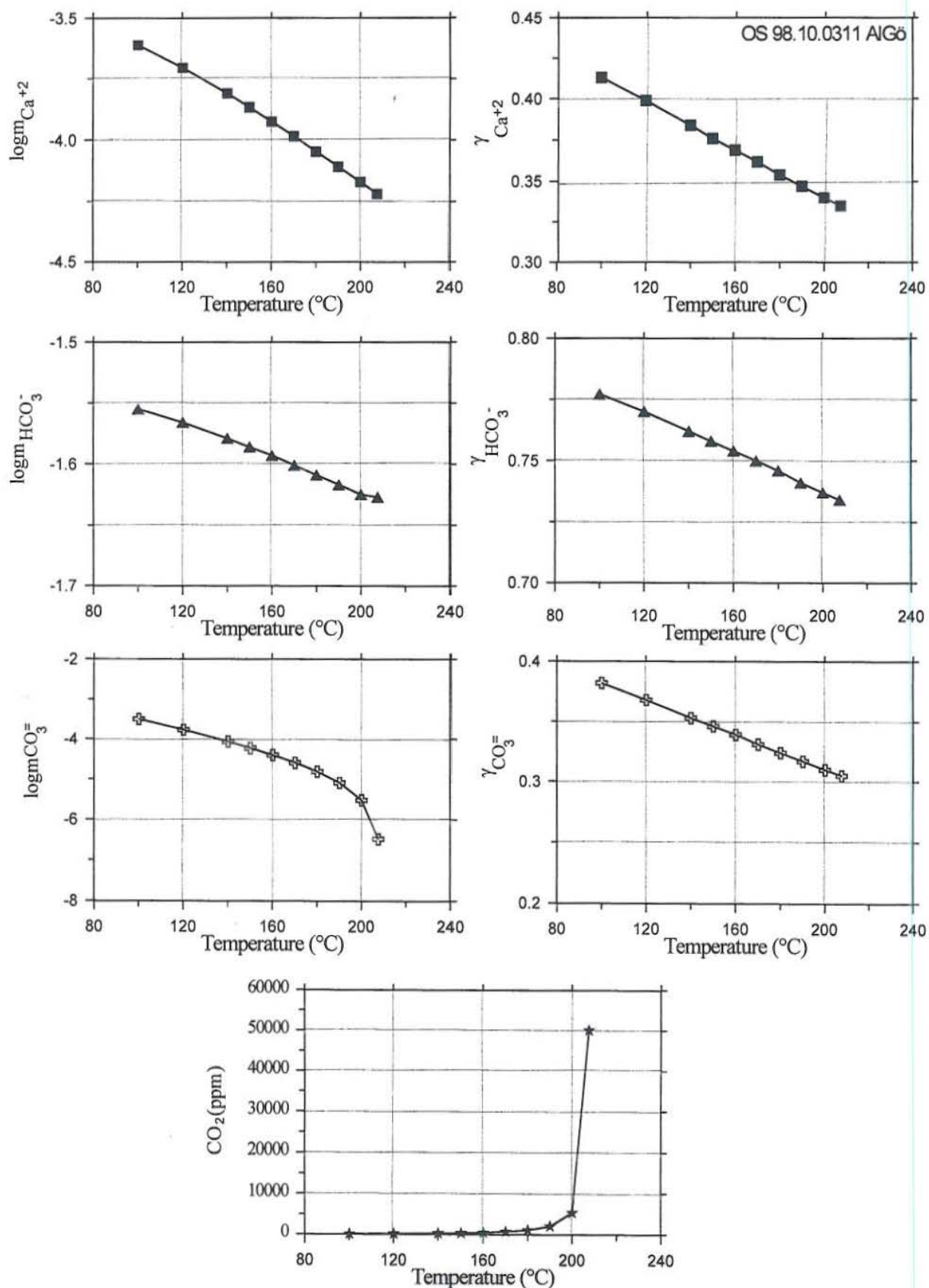


FIGURE 14: Changes in the concentrations (moles/kg) and activity coefficients ( $\gamma$ ) of calcium, bicarbonate and carbonate ions, and  $\text{CO}_2$  during one step adiabatic boiling of water for well KD-6

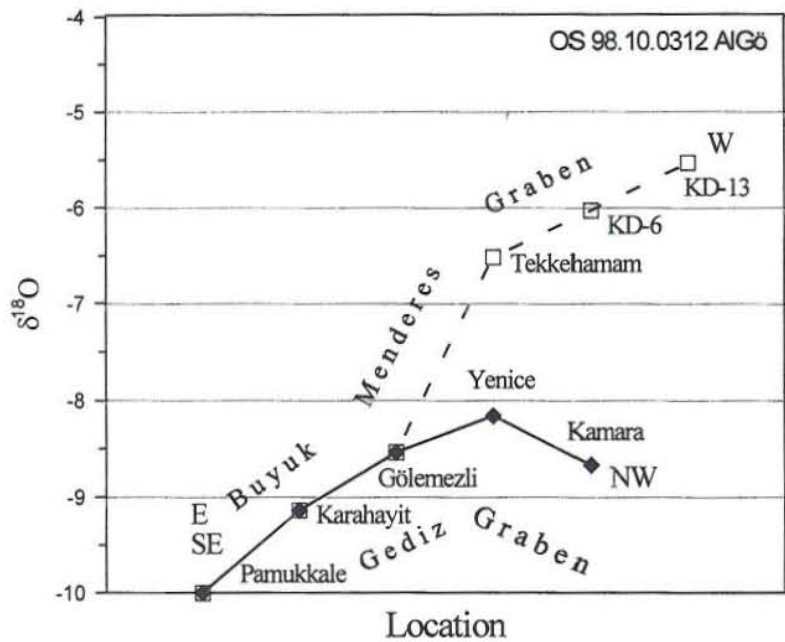


FIGURE 15: Location vs.  $\delta^{18}\text{O}$  values for geothermal waters from the study areas

Tekkehamam springs shows some oxygen-18 shift, but in water from other areas, little or no shift can be deduced (Figure 15). Water from Tekkehamam shows somewhat lower oxygen-18 shift than the Kizildere water. This lower oxygen-18 shift indicates correspondingly less water-rock interaction as compared to the Kizildere water. The meteoric water recharging the Kizildere and the Tekkehamam areas infiltrates to considerable depths while these depths appear to become progressively shallower from Kizildere to Pamukkale. The tritium content of the geothermal water varies between 14-28 and  $33 \pm 10$  TU (in 1979), indicating that they are older than 50 years (Filiz, 1982).

**The Cl-SO<sub>4</sub>-HCO<sub>3</sub> diagram:** In this triangular diagram, the data points for all waters plot close to the SO<sub>4</sub>-HCO<sub>3</sub> line (Figure 7). Water from well TH-1, Kizildere (No 1), Gebeler (2), Demirtaş (3), which is a boiling spring, İnalti (7), Babacık (8) and Gölemezli springs (see Table 3) are Na-SO<sub>4</sub>-HCO<sub>3</sub> waters. In the study areas the Pliocene rocks contain gypsum layers. Dissolution of gypsum from these layers will cause increasing sulphate concentrations in the water.

The study areas have been classified as CO<sub>2</sub>-rich discharge areas. Barnes et al. (1978) considered that CO<sub>2</sub> was derived from three different sources, organic material, metamorphism of marine carbonate rocks, and the mantle. They pointed out that  $\delta^{13}\text{C}$  isotope composition of mantle-derived CO<sub>2</sub> is in the range of -4.7 to -8.0‰. Analytical data on <sup>13</sup>C for some water in the area are in the range of -0.9 to -1.4‰ for Kizildere and Tekkehamam water, and -2.8 to -4.2‰ for Pamukkale, Kizilleğen and Kamara springs (Filiz, 1982). It is these isotopic data which have led to the conclusion that the origin of CO<sub>2</sub> in all the study areas is calcareous rocks which are undergoing metamorphism at depth. It is concluded that the relative abundance of SO<sub>4</sub> and HCO<sub>3</sub> in Turkish geothermal water in relation to Cl, is a reflection of the sedimentary rocks in these areas but not that this abundance reflects a peripheral or steam heated origin.

The Kizildere, Tekkehamam, Buldan, Pamukkale areas are located in an active earthquake zone. Most of the earthquakes originated in the eastern part of the Büyük Menderes graben. Outcrops of travertine in the area are common along tectonic lines (Figure 2). These tectonic fractures and the travertine are probably indications of periods of increased tectonic and seismic activity. The deep fractures act as paths for the ascending CO<sub>2</sub>.

### 5.2.2 Estimation of subsurface temperature

Subsurface temperatures in the study areas have been estimated by chemical geothermometry (Table 11). The quartz temperature calculated by WATCH gives a value of 176°C for well TH-1. Other quartz and chalcedony temperature equations, assuming steam loss is applied to the same sample, give values of 170-

171°C and 150-154°C, respectively. Quartz equilibrium temperatures for Kizildere springs lie in the range 150-180°C. For boiling springs at Tekkehamam the corresponding range is 140-170°C. By comparison with measured temperatures in drillholes at Kizildere it is concluded that subsurface temperatures in both areas must be quite similar.

TABLE 11: Results of different geothermometers for water in the study area  
(see Appendix II for equations)

No.	Tm	Quartz					Chalcedony				Na/K					Na-K-Ca <sup>#</sup>	Na-K-Ca
		1*	2	3	4	5	6	7	8	9	10	11	12	13	14	15	15
<b>Kizildere group</b>																	
W-1	92	165	-	201	-	201	-	190	-	182	186	216	194	231	182	253	253
1	100	146	-	149	-	148	-	128	-	126	179	210	186	225	174	210	228
2	100	175	-	178	-	177	-	162	-	157	172	205	180	221	167	208	215
<b>Tekkehamam group</b>																	
TH-1	116	176	-	171	-	170	-	154	-	150	188	217	195	232	184	65	214
3	98	178	-	168	-	167	-	150	-	146	153	189	162	206	147	65	178
4	99	141	-	141	-	141	-	119	-	118	183	213	190	229	179	167	214
5	60	174	183	171	178	170	163	154	157	150	209	234	215	248	207	67	190
6	72	157	165	156	159	155	142	136	138	134	188	218	196	233	185	92	207
7	55.5	226	227	206	227	206	215	197	203	189	187	216	194	232	183	88	187
8	61.5	161	161	153	154	152	137	132	134	130	179	210	187	226	174	51	172
9	73.5	178	183	171	178	170	163	154	157	150	181	211	189	227	177	205	207
<b>Buldan group</b>																	
10	36	135	137	133	128	132	110	109	109	109	419	380	406	379	446	16	257
11	40.8	137	137	133	128	132	110	109	109	109	246	262	250	274	248	111	190
12	56.8	147	148	141	139	141	122	119	120	118	235	253	239	266	235	106	201
<b>Pamukkale group</b>																	
13	35.5	85	85	88	72	86	54	59	56	61	216	239	222	253	215	60	144
14	59	94	95	97	83	95	64	69	66	71	252	267	256	278	255	69	174
15	28	113	113	112	102	111	84	86	84	87	241	258	245	270	242	53	158
16	54.5	91	91	93	79	91	60	65	62	67	264	275	266	286	268	62	178
17	50.4	166	166	156	159	156	142	137	138	134	195	223	202	238	192	48	179
18	48.4	148	149	142	141	141	123	120	121	119	182	212	190	228	178	29	172

\* Mg correction has been applied to the values (but not in the last column);  
(See Table 6 for the sources of the geothermometry equations used)

For the Buldan and Pamukkale springs, quartz equilibrium temperatures are generally in the range of 100-150°C. Due to the rather low temperatures in these areas, chalcedony equilibrium may be more appropriate, indicating that reservoir temperatures in these areas are 110-120°C or quite a bit lower than at Kizildere and Tekkehamam.

In the light of the geothermometry results for the Kizildere wells, the most appropriate calibration for the Na-K geothermometer is that of Arnórsson et al. (1983). For springs at Kizildere, it indicates subsurface temperatures of 180-186°C which is a little lower than was observed in drillholes. For springs from Tekkehamam this geothermometer indicates similar subsurface temperatures. Most values lie close to 190°C. It is, thus, concluded that subsurface temperatures at Tekkehamam are similar to those at Kizildere.

The Buldan group hot springs give Na-K temperatures which are much higher than either quartz or chalcedony equilibria. The cause is thought to be lack of equilibration with the feldspars. Accordingly, the Na-K geothermometry results are not reliable. The same applies to the Pamukkale group of springs.

The Na-K-Ca geothermometer indicates low reservoir temperatures for all areas, even lower than the measured temperature of the springs when Mg correction is applied. For Kizildere and Tekkehamam, uncorrected Na-K-Ca temperatures indicate that a Mg correction is not appropriate. They seem, on the other hand, to be valid for the warm springs at Buldan and Pamukkale. Here the Na-K-Ca geothermometer, when corrected for Mg, yields somewhat lower temperature than the silica geothermometer which can be accounted for by dissolution of Mg from the rock in the upflow.

In the Na-K-Mg triangular diagram, data points from the study area plot approximately on a line from the Mg-corner to the full equilibration line. The main cause of the linear variation is variable Mg content of the water. According to this diagram the Buldan and Pamukkale group water are immature to partly equilibrated, whereas the Tekkehamam and Kizildere waters have evolved more towards, or attained, full equilibrium.

### 5.2.3 Fluid/mineral equilibria

Figure 16 depicts mineral saturation ( $\log(Q/K)$ ) diagrams for boiling springs of Kizildere. As can be seen from the diagram, these springs are close to equilibrium with quartz and calcite at about 225°C. Figure 17 shows mineral equilibrium diagrams for the thermal springs at Tekkehamam. These diagrams indicate

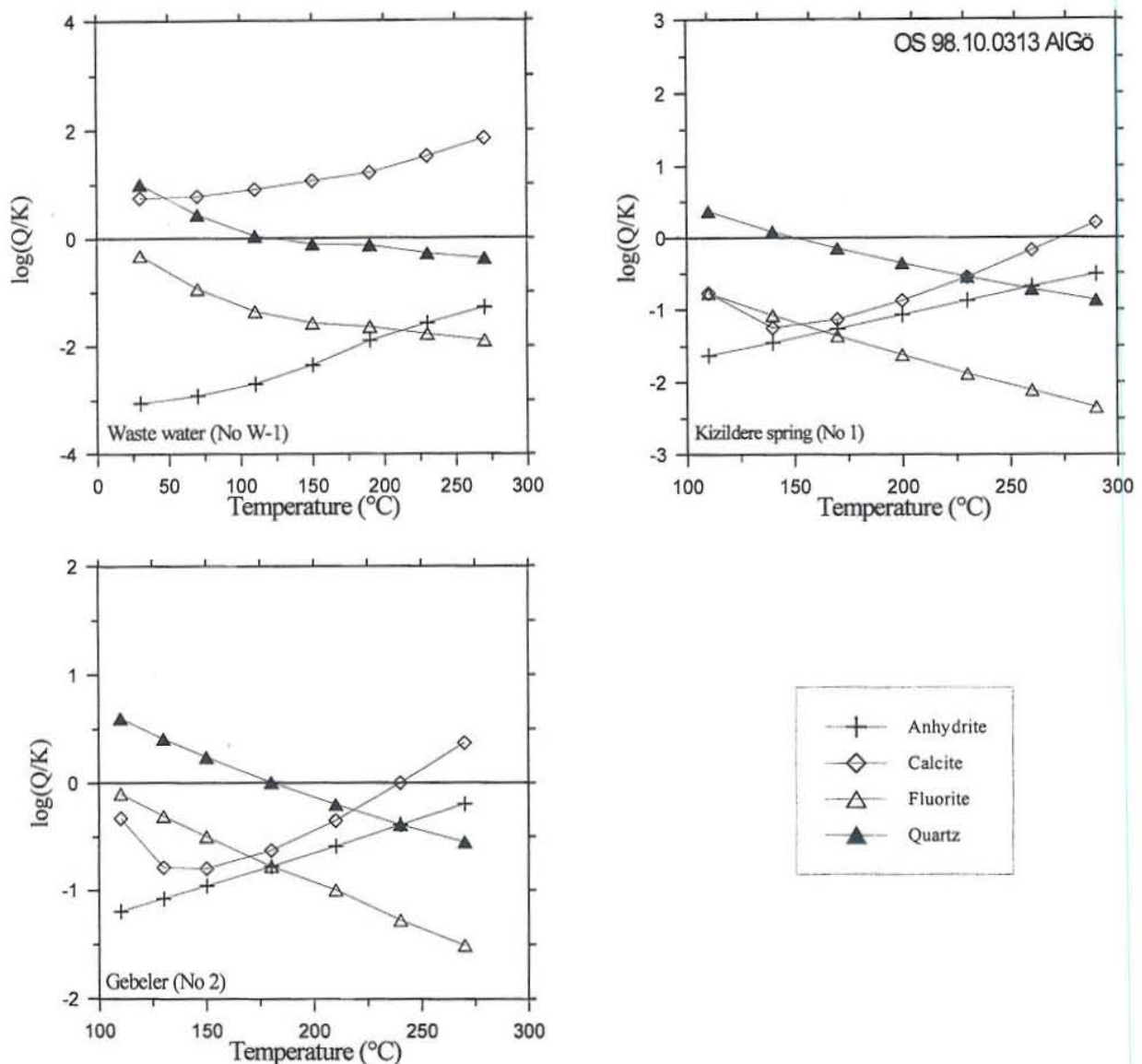


FIGURE 16: Mineral saturation  $\log(Q/K)$  diagrams for waste water and boiling springs of Kizildere

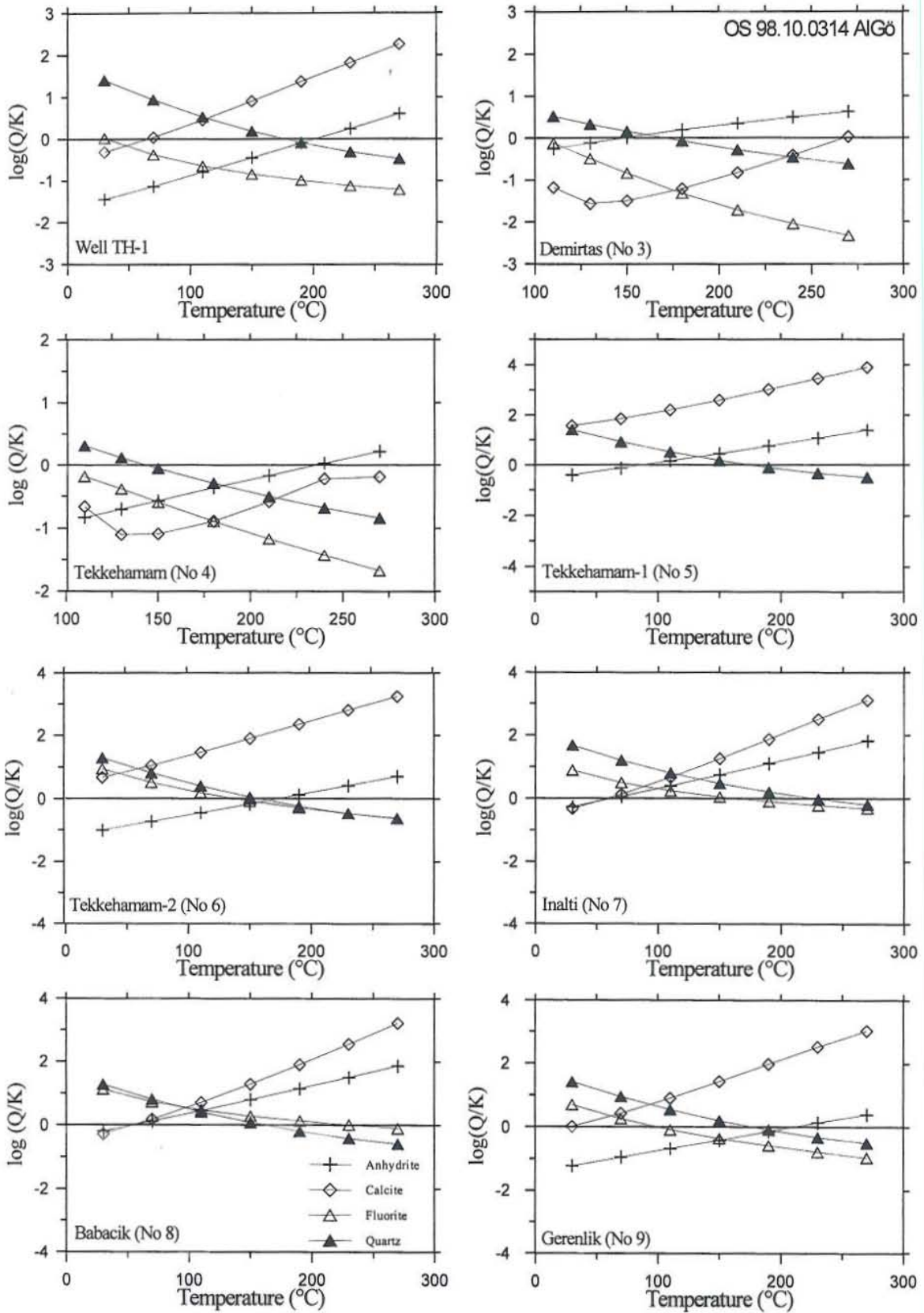


FIGURE 17: Mineral saturation log(Q/K) diagrams for the Tekkehamam group waters

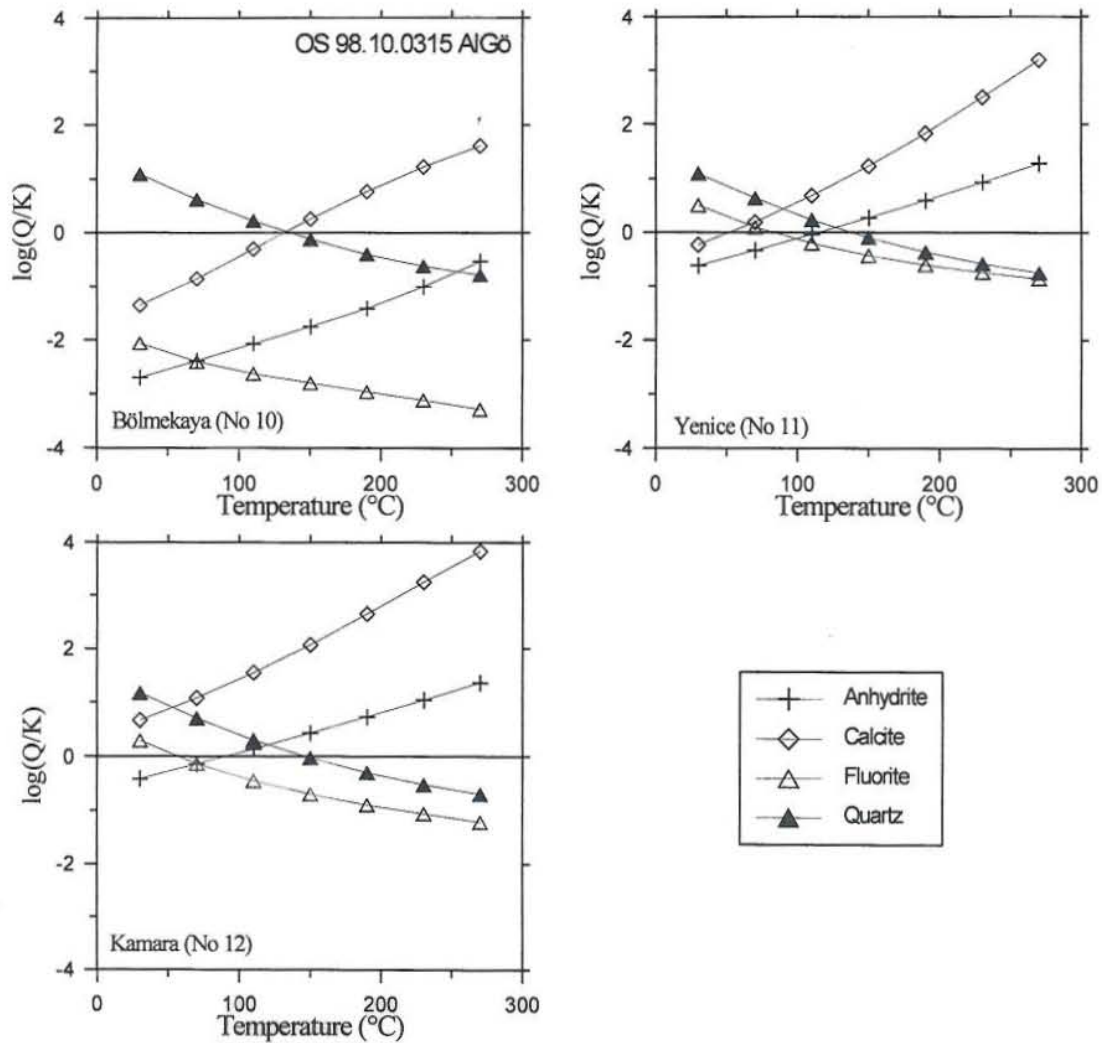


FIGURE 18: Mineral saturation  $\log(Q/K)$  diagrams for the Buldan group water

that the thermal water in Tekkehamam is close to equilibrium with quartz and anhydrite at a particular temperature which lies between 100 and 200°C and sometimes also with fluorite. At the equilibrium temperatures for these minerals, the Tekkehamam water is generally calcite supersaturated. Saturation for this mineral occurs at lower temperature. The cause is re-equilibration with this mineral in the upflow where the water cools. The diagrams of Figure 17 indicated that temperatures as high as 200°C are to be expected at Tekkehamam. The pattern for the Buldan and Pamukkale springs is comparable except that lower subsurface temperatures are indicated, generally 100-120°C (Figure 18 and 19).

The  $\log(Q/K)$  diagrams for the Pamukkale group of springs also include Na-, K-, Ca- and Mg-montmorillonite and albite curves. Adding these minerals does not change the overall picture.

#### 5.2.4 Evaluation of mixing processes

**Evidence for mixing:** As mentioned earlier in this report there is evidence that ascending hot water has mixed with cold water in upflow zones in the study areas. This evidence is the following:

1. Linear relationship between  $\delta^{18}\text{O}$  and chlorine (Figure 20). This relationship is thought to constitute particularly valuable evidence for mixing (Arnórsson, 1985).



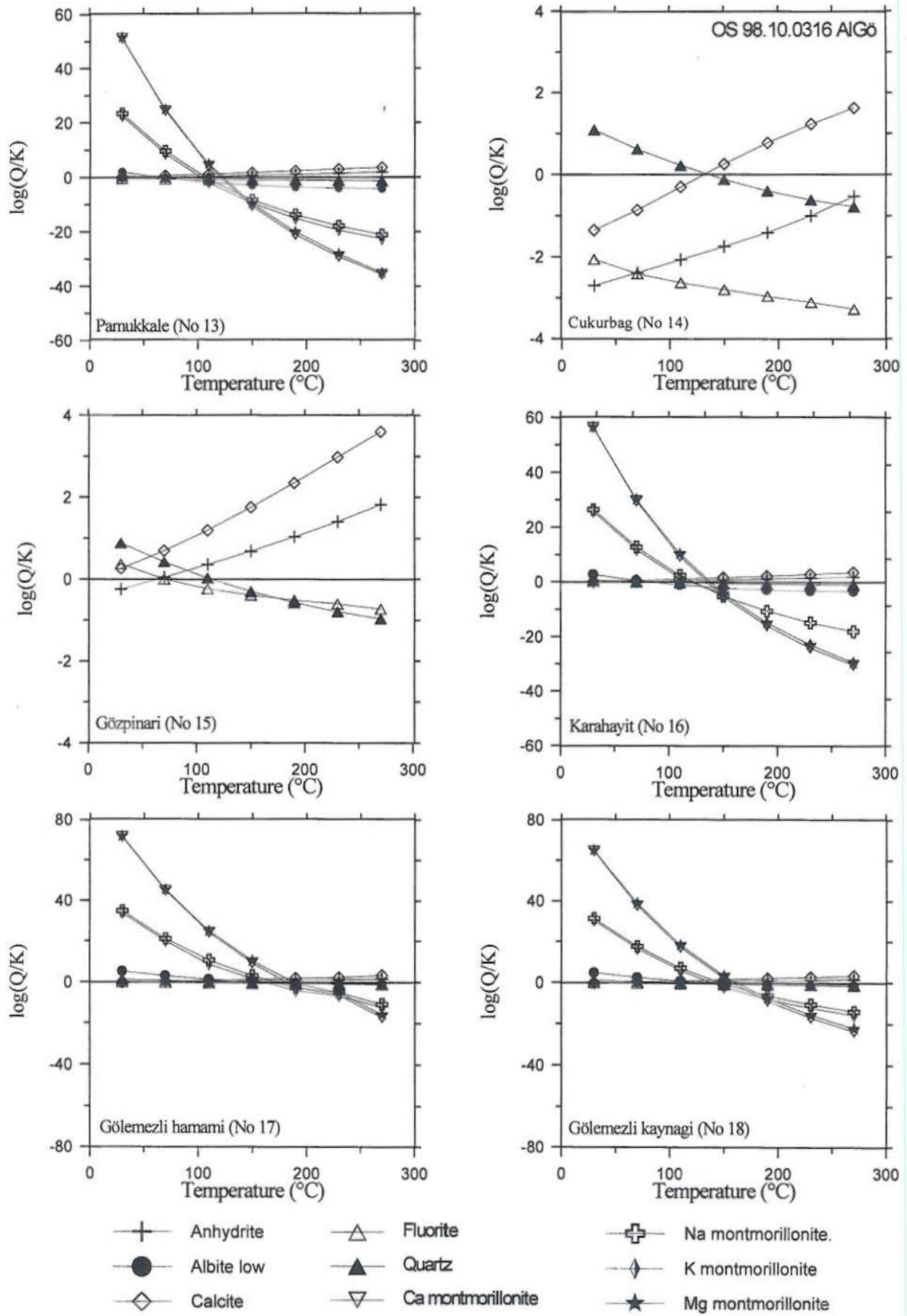


FIGURE 19: Mineral saturation log(Q/K) diagrams for the Pamukkale group waters

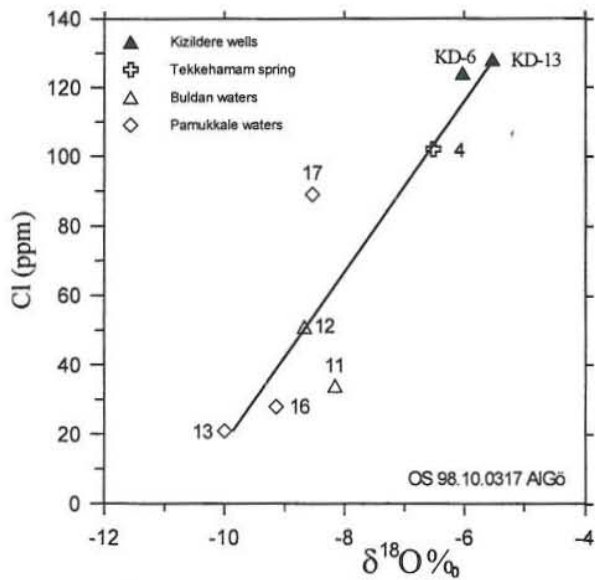
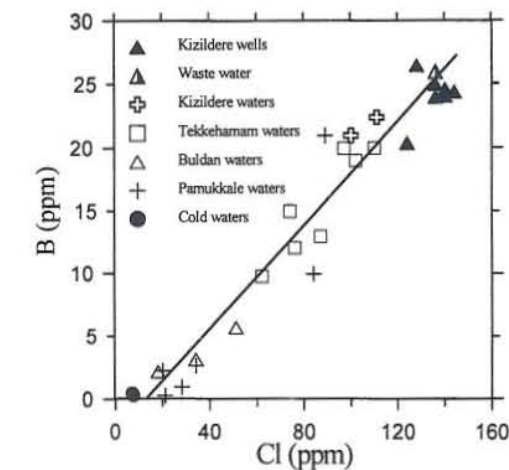


FIGURE 20: The linear relationship between  $\delta^{18}\text{O}$  and chloride



2. Linear relationship between Cl and B (Figure 21). A positive linear relationship between Cl and some other chemical constituents such as Na, F and  $\text{SiO}_2$  is also observed (Figure 21).
3. On the Na-K-Mg triangular diagram (Figure 9), samples 1, 2, 4 and 9 fall in the area of mixed water and all samples plot on a straight line from cold water to Kizildere wells.

Two **mixing models** were applied to the water in this study, the silica-enthalpy mixing model and the enthalpy-chlorine mixing model. Figure 22 depicts the **silica-enthalpy mixing model**. As expected, the Kizildere wells plot on the

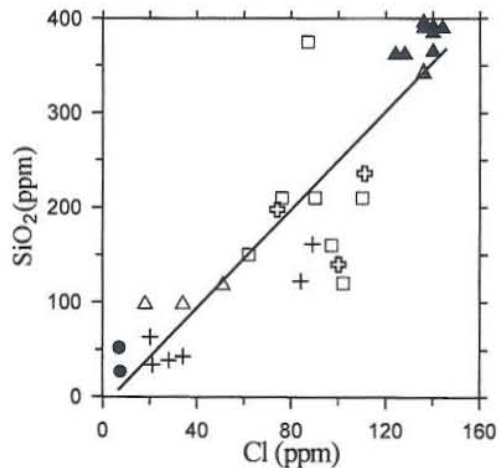
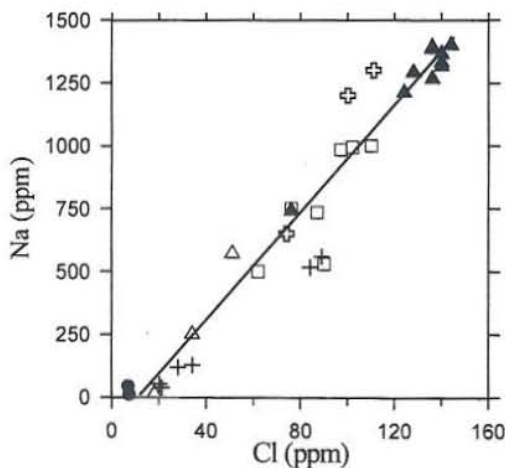
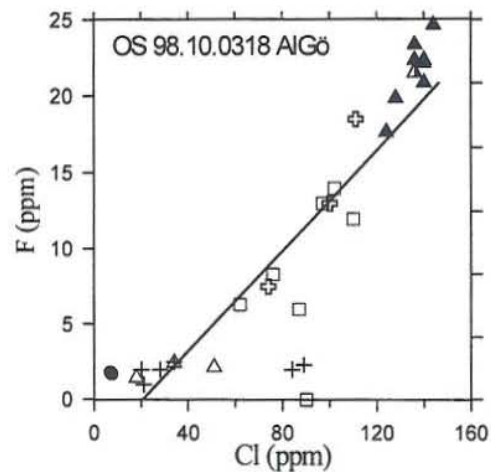


FIGURE 21: Relationship between Cl and some other constituents

maximum steam loss curve. Their location on this diagram corresponds to their quartz geothermometry temperature. The mixing lines a and b drawn through the data points for all the areas have a steep slope and they do not intersect at the quartz solubility curve. This suggests, at least in the case of sub-boiling

springs, that their water has cooled conductively in the upflow, thus causing a shift of the data points to the left on the diagram. Line a, which is drawn through data points 15, 11, 12, 8, 6 and 9 corresponds with the mixing of cold water with boiled geothermal water (point A). The temperature of the unboiled hot water component corresponding to A is found by drawing a horizontal line through point A to the quartz solubility curve corresponding to maximum steam loss. This gives 176°C for the hot water component. In the same way, mixing line b which connects cold water samples 15, 17, 18 and 5 gives a reservoir temperature of 195°C. Samples 13, 14 and 16 plot on the chalcedony solubility curve, but sample 5 plots on the amorphous silica solubility curve as does most of the water from the Pamukkale and Buldan groups. The high silica content of sample 7 may be due to inaccurate analysis.

**The chlorine-enthalpy mixing model** for this study is shown in Figure 23. It clearly shows two groups of water. Lines a and b, which represent mixing, connect cold water, Gölemezli springs at Pamukkale, TH-1 and some springs from Tekkehamam and Kizildere. These mixing lines give the reservoir temperature in the range 203-222°C. Lines c and d, which connect samples from Buldan and Pamukkale, indicate temperatures of 110 and 149°C, respectively, for the hot water component.

## 6. CONCLUSIONS

The main task of this study was to estimate subsurface temperatures in the Kizildere and neighbouring geothermal fields and to assess boiling processes in wells at Kizildere in order to understand the scaling problems. The main conclusions and results of the study are as follows:

1. The Kizildere and Tekkehamam group water is of the Na-HCO<sub>3</sub>-SO<sub>4</sub> type whereas the type of water in the Buldan and Pamukkale geothermal fields varies from Na-, Ca- and Mg-HCO<sub>3</sub> to Ca-Mg-HCO<sub>3</sub>-SO<sub>4</sub> types.
2. The origin of all the water in the study area is meteoric.
3. The relative abundance of SO<sub>4</sub> and HCO<sub>3</sub> in the Kizildere water in relation to Cl is a reflection of the sedimentary rocks in this area.
4. The average reservoir temperature, which is 206°C for the Kizildere wells, calculated with Na-K

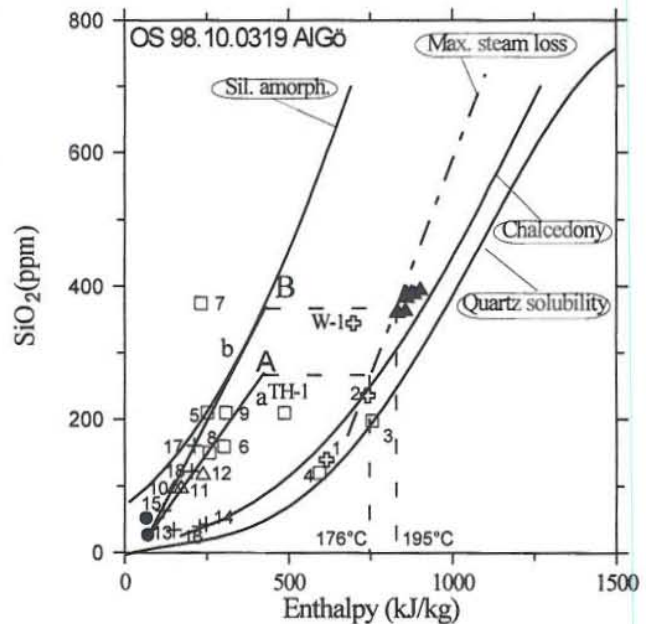


FIGURE 22: The silica-enthalpy mixing model for water from the study area

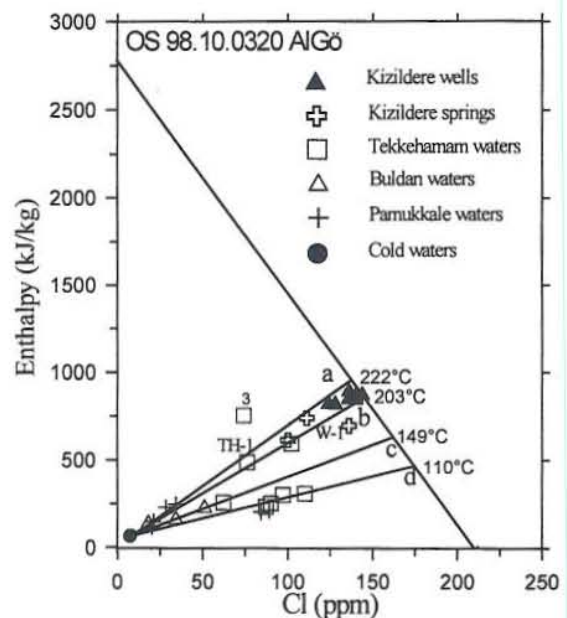


FIGURE 23: The enthalpy-chlorine mixing model for water from the study area

geothermometry equations is very close to the measured aquifer temperature. This is taken to indicate that the Kizildere reservoir water is close to equilibrium with alkali feldspars. The average Na-K-Ca temperature is obtained 245°C for these wells. Part of this difference could be due to imprecise calibration of this geothermometer or be an indication of higher temperatures at deeper levels.

5. Kizildere water is fully equilibrated whereas Pamukkale, Buldan and Tekkehamam water is immature to partly equilibrated. The meteoric water recharging the Kizildere and the Tekkehamam areas infiltrates to considerable depths while these depths appear to become progressively shallower from Kizildere to Pamukkale.
6. Ascending hot water is mixed with cold water in upflow zones. The mixing models applied to water in the study area give reservoir temperatures ranging between 110 and 222°C.
7. The boiled water from Kizildere wells is supersaturated with respect to calcite even at low temperatures. The reason for this is a strong increase in  $\text{CO}_3^{2-}$  concentration due to  $\text{CO}_2$  degassing and the disintegration of the  $\text{CaHCO}_3^+$  ion pair which causes free  $\text{Ca}^{+2}$  concentrations to increase.

#### ACKNOWLEDGEMENTS

I would like to express my gratitude to Dr. Ingvar Birgir Fridleifsson and Mr. Lúdvík S. Georgsson for making it possible for me to attend the UNU Geothermal Training Programme, and for their technical advice and moral support during the whole training period. Special thanks are due to Professor Stefán Arnórsson, my advisor, for sharing his experience and his excellent guidance during all stages of preparing this report. I am grateful to Dr. Jón Örn Bjarnason for his help and valuable discussions. My thanks go to Professor Sakir Simsek, Dr. İ. Hakki Karamanderesi, Dr. Halil Kumsar, Dr. Halldór Ármannsson and Dr. Benedikt Steingrímsson for providing data on the chemical analyses of water and background information which were very useful during all stages of writing this report. I also thank all the lecturers and staff members at Orkustofnun, for their excellent presentations and willingness to share their knowledge and experience. I express my hearty thanks to Mrs. Guðrún Bjarnadóttir for her special help and arrangement during the training programme.

#### REFERENCES

- Alptekin, O., 1973: *Focal mechanism of earthquakes in western Turkey and their tectonic implications*. Ph.D. Thesis, Institute of Mining and Technology, Socopro, New Mexico.
- Altunel, E., 1996: The morphological features, ages and neotectonic importance of Pamukkale travertines. *M.T.A. Journal (in Turkish), Ankara, 118, 47-64*.
- Arnórsson, S., 1975: Application of the silica geothermometer in low-temperature hydrothermal areas in Iceland. *Am. J. of Sci.*, 275, 763-783.
- Arnórsson, S., 1985: The use of mixing models and chemical geothermometers for estimating underground temperature in geothermal systems. *J. Volc. Geotherm. Res.*, 23, 299-335.
- Arnórsson, S., Gunnlaugsson, E., and Svavarsson, H., 1983: The chemistry of geothermal waters in

Iceland III. Chemical geothermometry in geothermal investigations. *Geochim. Cosmochim. Acta*, 47, 567-577.

Arnórsson, S., Sigurdsson, S. and Svavarsson, H., 1982: The chemistry of geothermal waters in Iceland I. Calculation of aqueous speciation from 0°C to 370°C. *Geochim. Cosmochim. Acta*, 46, 1513-1532.

Arpat, E., and Bingöl, E., 1969: Considerations on the graben system in the Aegean Region. *M.T.A. Journal (in Turkish)*, Ankara, 73, 1-9.

Barnes, I., Irwin, W.P. and White, D.E. 1978: *Global distribution of carbon dioxide discharges and major zones of seismicity*. U.S. Geological Survey, Water Resources Investigations, report 78-39, 12 pp.

Bingöl, E., 1976: The geotectonic evolution of the West Anatolia. *M.T.A. Journal (in Turkish)*, Ankara, 86, 14-35.

Bjarnason, J.Ö., 1994: *The speciation program WATCH, version 2.1*. Orkustofnun, Reykjavík, 7 pp.

Craig, H., 1961: Standards for reporting concentrations of deuterium and oxygen-18 in natural waters. *Science* 133, 1833-1834.

Demirörer, M., 1967: *Gradient studies in the Denizli-Saraykoy area*. M.T.A., Ankara, Report No. 4141 (in Turkish).

Durak, S., Erkan, B. and Aksoy, N., 1993: Calcite removal from wellbores at Kizildere geothermal field, Turkey. *Proceedings of the 15<sup>th</sup> New Zealand Geothermal Workshop*, 11-15.

Ekingen, A., 1970: *Gravity study of the Denizli-Saraykoy area*. M.T.A., Ankara, report No. 4788 (in Turkish).

ENEL, Aquater, DAL and Geotermica Italiana, 1989: *Optimization and development of the Kizildere geothermal field*. ENEL, Aquater, DAL and Geotermica Italiana, Pisa, Italy, final report.

Ercan, T., 1979: The Senozoic volcanism in the West of Turkey, the Aegean Islands and Thrace. *Geological Engineering (in Turkish)*, Ankara, 9, 23-46.

Filiz, S., 1982: *The investigation by <sup>18</sup>O, <sup>2</sup>H, <sup>3</sup>H ve <sup>13</sup>C isotopes of the important geothermal areas in the Aegean Region*. Ass. Prof. thesis at Aegean University ( in Turkish), Earth and Sci. fac., İzmir , 95 pp.

Fournier, R.O., 1973: Silica in thermal waters. Laboratory and field investigations. *Proceedings of the International Symposium on Hydrogeochemistry and Biochemistry, Tokyo, 1, Clark Co., Washington D.C.*, 122-139.

Fournier, R.O., 1977: Chemical geothermometers and mixing model for geothermal systems. *Geothermics*, 5, 41-50.

Fournier, R.O., 1979: A revised equation for Na-K geothermometer. *Geoth. Res. Council, Transactions*, 3, 221-224.

Fournier, R.O., 1991: Water geothermometers applied to geothermal energy. In: D'Amore, F. (coordinator), *Application of Geochemistry in Geothermal Reservoir Development*. UNITAR/UNDP publication, Rome, 37-69.

Fournier, R.O., and Potter, R.W. II, 1979: Magnesium correction to the Na-K-Ca chemical geothermometer. *Geochim. Cosmochim. Acta*, 43, 1543-1550.

Fournier, R.O., and Potter, R.W. II, 1982: A revised and expanded silica (quartz) geothermometer. *Geoth. Res. Council Bull.*, 11-10, 3-12.

Fournier, R.O., and Rowe, J.J., 1966: Estimation of underground temperatures from the silica contents of water from hot springs and wet steam wells. *Am. J. Sci.*, 264, 685-697.

Fournier, R.O., and Rowe, J.J., 1977: The solubility of amorphous silica in water at high temperatures and high pressures. *Am. Min.*, 62, 1052-1056.

Fournier, R.O., and Truesdell, A.H., 1973: An empirical Na-K-Ca geothermometer for natural waters. *Geochim. Cosmochim. Acta*, 37, 1255-1275.

Giese, L.B., Pekdeğer, A. and Dams, E., 1998: Thermal fluids and scalings in the geothermal power plant of Kizildere, Turkey. *Proceedings of the 9<sup>th</sup> International Symposium on Water-Rock Interaction, Taupo, New Zealand*, A.A. Balkema, Rotterdam, 625-628.

Giggenbach, W.F., 1988: Geothermal solute equilibria. Derivation of Na-K-Mg-Ca geothermometers. *Geochim. Cosmochim. Acta*, 52, 2749-2765.

Giggenbach, W.F., 1991: Chemical techniques in geothermal exploration. In: D'Amore, F. (coordinator), *Application of geochemistry in geothermal reservoir development*, UNITAR/UNDP publication, Rome, 119-142.

Giggenbach, W.F., Gonfiantini, R., Jangi, B.L, and Truesdell, A.H., 1983: Isotopic and chemical composition of Parbati valley geothermal discharges, NW-Himalaya, India. *Geothermics*, 12, 199-222.

Gökgöz, A., 1994: *Hydrogeology of Pamukkale-Karahayıit-Gölemezli hydrothermal Karst system*. Ph.D. Thesis (in Turkish), Süleyman Demirel University, Engineering faculty, Isparta, 263 pp.

Gülec, N., 1988: The distribution of helium-3 in West Turkey. *M.T.A. Journal (in Turkish)*, Ankara, 108, 98-105.

Kaya, O., 1981: The underthrust of western Anatolia: The geological situation of the Menderes massif and ultramafic unit. *Nature Journal (in Turkish)*, Ankara, *Ataturk special edition.*, 15-36.

Líndal, B. and Kristmannsdóttir, H., 1989: The scaling properties of the effluent water from Kizildere power station, Turkey, and recommendation for a pilot plant in view of district heating applications. *Geothermics*, 18-1/2, 217-223.

Mahon, W.A.J., 1970: Chemistry in the exploration and exploitation of hydrothermal systems. *Geothermics*, Sp. issue 2-2, 1310-1322.

Mertoğlu, O., Mertoğlu, F.M. and Basarir, N.H., 1993: The experience on preventing scaling and corrosion problems and their contribution to geothermal development in Turkey. *Communications of the International Symposium: Geothermics '94 in Europe, Orléans, France, BRGM 230*, 497-503.

Okandan, E., 1988: An analysis of natural state of Kizildere field, Turkey. In: Okandan, E. (editor), *Geothermal reservoir engineering*. NATO ASI Series, Kluwer Academic Publishers, Dordrecht, 213-222.

- Özgür, N., Vogel, M., and Pekdeğer, A., 1998: A new type of hydrothermal alteration at the Kizildere geothermal field in the rift zone of the Büyük Menderes, western Anatolia, Turkey. *Proceedings of the 9<sup>th</sup> International Symposium on Water-Rock Interaction, Taupo, New Zealand*, A.A. Balkema, Rotterdam, 679-682.
- Reed, M.H., and Spycher, N.F., 1984: Calculation of pH and mineral equilibria in hydrothermal water with application to geothermometry and studies of boiling and dilution. *Geochim. Cosmochim. Acta*, 48, 1479-1490.
- Rimstidt, J.D., and Barnes, H.L., 1980: The kinetics of silica-water reactions. *Geochim. Cosmochim. Acta*, 44, 1683-1699.
- Sengör and Yilmaz, 1981: Tethyan evaluation of Turkey: A plate tectonic approach. *Tectonophysics*, 75, 181-241.
- Simsek, S., 1982: *Geology and geothermal energy possibilities of the Denizli-Sarayköy-Buldan area*. Ph.D. Thesis, Istanbul University, Earth and Sciences Faculty, Istanbul.
- Simsek, S., 1985a: Geothermal model of Denizli-Saraykoy-Buldan area. *Geothermics*, 14-2/3, 393-417.
- Simsek, S., 1985b: Present status and future development of the Denizli-Kizildere geothermal field of Turkey. *1985 International Symposium on Geothermal Energy, Geoth. Res. Council, international volume*, 203-210.
- Simsek, S. and Yilmazer, S., 1977: *Geology and geothermal energy possibilities of the Nazilli-Kuyucak-Yenice (Karacasu) area*. M.T.A., Ankara, report No. 6390 (in Turkish).
- Tan, E., 1985: Reservoir characteristics of the Kizildere geothermal field. *Geothermics*, 14-2/3, 419-428.
- Tezcan, A.K., 1967: *Investigations on geothermal energy, gravity and resistivity in the Denizli-Sarayköy area*. M.T.A., Ankara, report No. 3896 (in Turkish).
- Tezcan, A. K., 1979: Geothermal studies, their present status and contribution to heat flow contouring in Turkey. Springer, Berlin.
- Toksöz, N., 1975: Subduction of the lithosphere. *Sci. Am.*, 233, 89-101.
- Tonani, F., 1970: Geochemical methods of exploration for geothermal energy. *Geothermics, Sp. issue*, 2-1, 492-515.
- Truesdell, A.H., 1976: Summary of section III - geochemical techniques in exploration. *Proceedings of the 2nd U.N. Symposium on the Development and Use of Geothermal Resources, San Francisco*, 1, liii-lxxix.
- Truesdell, A.H., and Hulston, J.R., 1980: Isotopic evidence of environments of geothermal systems, In: Fritz, P., and Fontes, J.C., (editors), *Handbook of Environmental Isotope Chemistry*. Elsevier, New York, 179-226.
- White, D.E., 1970: Geochemistry applied to the discovery, evaluation, and exploration of geothermal energy resources. *Geothermics, Sp. issue*, 2-1, 58-80.
- Yildirim, N., Demirel, Z. and Doğan, A.U., 1997: Geochemical characteristic and re-injection of the Kizildere-Tekkehamam geothermal field. *GEOENV'97, Istanbul, abstracts*, 48.

### APPENDIX I: Calculation of total carbonate as $CO_2$

The calculation method involves calculating the equivalent concentrations of the interfering bases in solution from their analysis and the pH measurement. Solution is theoretically titrated from pH=8.2 (at this pH the  $HCO_3$  anion has all been converted to  $CO_2$ ) to pH=4.5. The interference of acids from boron and silica is corrected. Calculation is based on the following equation:

$$CO_2 = \frac{\text{titrex Ax 4400}}{\text{ml sample}} - (6.97 + 1.182 \times H_2S + 0.0088 \times SiO_2 + 0.100 \times B)$$

where  $CO_2$  represents total carbonate in ppm. Other component concentrations in the equation are also in ppm.

### APPENDIX II: Equations for silica and cation geothermometers (concentrations in ppm)

#### Quartz geothermometers

##### 1. Fournier and Potter (1982)

$$t^{\circ}C = C_1 + C_2S + C_3S^2 + C_4S^3 + C_5 \log S \quad (1)$$

where  $C_1 = -4.2198 \times 10^1$ ,  $C_2 = 2.8831 \times 10^{-1}$ ,  $C_3 = -3.6686 \times 10^{-4}$ ,  
 $C_4 = 3.1665 \times 10^{-7}$ ,  $C_5 = 7.7034 \times 10^1$ ,  $S = SiO_2$

##### 2. No steam loss (Fournier, 1973)

$$t^{\circ}C = \frac{1309}{5.19 - \log SiO_2} - 273.15 \quad (2)$$

##### 3. Maximum steam loss at 100°C (Fournier, 1973)

$$t^{\circ}C = \frac{1522}{5.75 - \log SiO_2} - 273.15 \quad (3)$$

##### 4. No steam loss (Arnórsson et al., 1983)

$$t^{\circ}C = \frac{1164}{4.90 - \log SiO_2} - 273.15 \quad (4)$$

##### 5. Maximum steam loss at 100°C (Arnórsson et al., 1983)

$$t^{\circ}C = \frac{1498}{5.70 - \log SiO_2} - 273.15 \quad (5)$$



**Chalcedony geothermometers**

6. No steam loss (Fournier, 1973)

$$t^{\circ}\text{C} = \frac{1032}{4.69 - \log\text{SiO}_2} - 273.15 \quad (6)$$

7. Maximum steam loss at 100°C (Fournier, 1973)

$$t^{\circ}\text{C} = \frac{1182}{5.09 - \log\text{SiO}_2} - 273.15 \quad (7)$$

8. No steam loss (Arnórsson et al., 1983)

$$t^{\circ}\text{C} = \frac{1112}{4.91 - \log\text{SiO}_2} - 273.15 \quad (8)$$

9. Maximum steam loss at 100°C (Arnórsson et al., 1983)

$$t^{\circ}\text{C} = \frac{1264}{5.31 - \log\text{SiO}_2} - 273.15 \quad (9)$$

**Na/K geothermometers**

10. Truesdell (1976)

$$t^{\circ}\text{C} = \frac{856}{0.857 + \log(\text{NA/K})} - 273.15 \quad (10)$$

11. Fournier (1979)

$$t^{\circ}\text{C} = \frac{1217}{1.483 + \log(\text{NA/K})} - 273.15 \quad (11)$$

12. Arnórsson et al., (1983)

$$t^{\circ}\text{C} = \frac{933}{0.993 + \log(\text{NA/K})} - 273.15 \quad (12)$$

13. Giggenbach (1988)

$$t^{\circ}\text{C} = \frac{1390}{1.75 + \log(\text{NA/K})} - 273.15 \quad (13)$$

14. Fournier and Truesdell (1973)

$$t^{\circ}\text{C} = \frac{777}{0.70 + \log(\text{NA/K})} - 273.15 \quad (14)$$

### Na-K-Ca geothermometer

Fournier (1973)

$$t^{\circ}\text{C} = \frac{1647}{\log(\text{NA/K}) + \beta [\log(\sqrt{\text{Ca/Na}}) + 2.06] + 2.47} - 273.15 \quad (15)$$

where  $\beta = 4/3$  for  $t < 100^{\circ}\text{C}$ , and  $\beta = 1/3$  for  $t > 100^{\circ}\text{C}$

Magnesium correction to the Na-K-Ca geothermometer:

$$R = \frac{C_{Mg}}{C_{Mg} + 0.61 C_{Ca} + 0.31 C_K} \times 100 \quad (16)$$

In the equations  $C_x$  and  $T$  represent the concentration of component  $x$  in ppm and Na-K-Ca temperature in K, respectively.

For  $1.5 < R < 5$  the Mg correction,  $\Delta t_{Mg}$  ( $^{\circ}\text{C}$ ) is:

$$\Delta t_{Mg} = -1.03 + 59.971 \times \log R + 145.05 \times (\log R)^2 - 36711 \times (\log R)^2 / T - 1.67 \times 10^7 \times \log R / T^2$$

For  $5 < R < 50$

$$\Delta t_{Mg} = 10.66 - 4.7415 \times \log R + 325.87 \times (\log R)^2 - 1.032 \times 10^5 (\log R)^2 / T - 1.968 \times 10^7 \times \log R / T^2 + 1.605 \times 10^7 \times (\log R)^3 / T^2$$

Do not apply a Mg correction if  $\Delta t$  is negative or  $R < 1.5$ .